SEDRA MOHAMEED

COMPARİSON OF INTRACRANİAL HEMORRHAGES DETECTİON PERFORMANCES OF DEEP LEARNİNG MODELS ON CT IMAGES

MASTER THESIS

2025

NEAR EAST UNIVERSITY

INSTITUTE OF GRADUATE STUDIES

DEPARTMENT OF BIOMEDICAL ENGINEERING

COMPARISON OF INTRACRANIAL HEMORRHAGES DETECTION PERFORMANCES OF DEEP LEARNING MODELS ON CT IMAGES

M.Sc. THESIS

Sedra MOHAMEED

Nicosia

January, 2025

NEAR EAST UNIVERSITY
INSTITUTE OF GRADUATE STUDIES
DEPARTMENT OF BIOMEDICAL ENGINEERING

COMPARİSON OF INTRACRANİAL HEMORRHAGES DETECTİON PERFORMANCES OF DEEP LEARNİNG MODELS ON CT IMAGES

M.Sc. THESIS

Sedra MOHAMEED

Supervisor
Assist. Prof. Dr. Omid MIRZEAI
Dr. Ahmet İLHAN

Nicosia
January, 2025

Approval

We certify that we have read the thesis submitted by Sedra Ali-alsagher Mohammed **titled "Comparison of Intracranial Hemorrhage Detection Performances of Deep Learning Models on CT Images"** and that in our combined opinion it is fully adequate, in scope and in quality, as a thesis for the degree of Master of Biomedical Engineering Sciences.

Examining Committee	Name-Surname	Signature
Head of the Committee:	Assoc. Prof. Dr. Boran Şekeroğlu	
Committee Member:	Assist. Prof. Dr. Elbrus Bashir İMANOV	
Supervisor:	Assist. Prof. Dr. Omid MIRZEAI	
Co-Supervisor:	Dr. Ahmet İLHAN	

Approved by the Head of the Department

24/01/2025

Assoc. Prof. Dr. Süleyman Aşır

Head of the Department

Approved by the Institute of Graduate Studies

24/01/2025

Prof. Dr. Kemal Hüsnü Can Başer

Head of the Institute of Graduate Studies

Declaration of Ethical Principles

I hereby declare that all information, documents, analysis and results in this thesis have been collected and presented according to the academic rules and ethical guidelines of Institute of Graduate Studies, Near East University. I also declare that as required by these rules and conduct, I have fully cited and referenced information and data that are not original to this thesis.

Sedra MOHAMEED

24/01/2025

Acknowledgments

"The teacher seemed like a divine messenger". How true these words are. I would like to thank my supervisor Assist. Prof. Dr. Omid MIRZEAI for his guidance, encouragement and patience. I also express my gratitude to my co-supervisor Dr. Ahmet İLHAN for his support, effort and guidance throughout my studies for this thesis. I would like to express my gratitude and appreciation to Assoc. Prof. Dr. Boran Şekeroğlu for his endless support and advice.

I am equally grateful to my university as a whole and my department in particular for enabling the test runs of my software that required considerable processing power.

Finally, I would like to thank my family for their endless patience, solidarity and inspirational support during this research. And with a grateful heart, I am especially thankful to BME. Zain Al-abideen for his loyal support and trust in me, which have been instrumental in the successful completion of my thesis.

Sedra MOHAMEED

Abstract

Comparison of Intracranial Hemorrhages Detection Performances of Deep Learning Models on CT Images

MOHAMEED Sedra
M.Sc., Department of Biomedical Engineering
January, 2025, 55 pages

Early detection of Intracranial hemorrhage (ICH) is crucial to prevent life-threatening conditions and mortality. Computed Tomography (CT) is the primary imaging system used to diagnose intracranial hemorrhages, which provides distinct differences between epidural, subdural, and subarachnoid pleurae. However, the occurrence of ICH could be indistinct and might cause misdiagnosis. Recent advancements in Artificial Intelligence (AI) and deep learning technologies provide effective and rapid analysis of low and high-level features of images, even though the appearance of the region of interest is indistinct. This efficacy of the deep learning methods is also improved by transferring the knowledge obtained in another domain to different tasks. In this thesis, we implemented three state-of-the-art pretrained deep learning models, EfficientNetB0, DenseNet201, and ResNet101, using a transfer learning approach to detect ICH in order to help and assist medical doctors. The DenseNet201 outperformed ResNet101 and EfficientNet B0 models and achieved 0.8076, 0.8451, and 0.981 Sensitivity, F1, and ROC AUC scores. The results showed that deep learning models can be used to detect ICH accurately; however, further improvements are required to increase the sensitivity.

Keywords*:* intracranial hemorrhage, brain bleeding, hemorrhagic stroke, ct imaging, neurosurgery

Özet

BT Görüntülerinde Derin Öğrenme Modellerinin İntrakranial Kanama Tespit Performanslarının Karşılaştırılması

MOHAMEED Sedra
Yüksek Lisans, Biyomedikal Mühendisliği Bölümü
Ocak, 2025, 55 sayfa

Kafatası içi kanamanın (ICH) erken teşhisi, yaşamı tehdit eden durumları ve ölüm oranını önlemek için çok önemlidir. Bilgisayarlı Tomografi (BT), kafatası içi kanamaları teşhis etmek için kullanılan birincil görüntüleme sistemidir ve epidural, subdural ve subaraknoid plevralar arasındaki belirgin farklılıkları sağlar. Ancak, ICH'nin oluşumu belirsiz olabilir ve yanlış tanıya neden olabilir. Yapay Zeka (AI) ve derin öğrenme teknolojilerindeki son gelişmeler, ilgi alanının görünümü belirsiz olsa bile, görüntülerin düşük ve yüksek seviyeli özelliklerinin etkili ve hızlı bir şekilde analiz edilmesini sağlar. Derin öğrenme yöntemlerinin bu etkinliği, başka bir alanda elde edilen bilginin farklı görevlere aktarılmasıyla da artırılır. Bu tezde, tıp doktorlarına yardımcı olmak ve desteklemek amacıyla ICH'yi tespit etmek için bir transfer öğrenme yaklaşımı kullanarak, EfficientNetB0, DenseNet201 ve ResNet101 olmak üzere üç adet son teknoloji önceden eğitilmiş derin öğrenme modeli uyguladık. DenseNet201, ResNet101 ve EfficientNet B0 modellerinden daha iyi performans gösterdi ve 0,8076, 0,8451 ve 0,981 Duyarlılık, F1 ve ROC AUC puanlarına ulaştı. Sonuçlar, derin öğrenme modellerinin ICH'yi doğru bir şekilde tespit etmek için kullanılabileceğini gösterdi; ancak duyarlılığı artırmak için daha fazla iyileştirmeye ihtiyaç var.

Anahtar kelimeler: İntrakraniyal kanama, Beyin kanaması, Hemorajik inme, BT görüntüleme, Nöroşirürji

Table of Contents

List of Tables

List of Figures

List of Abbreviations

AI: Artificial Intelligence

ANN: Artificial Neural Network

AUC: Area Under the Curve

CAD: Computer-Aided Diagnosis

CNN: Convolutional Neural Network

CSF: Cerebrospinal Fluid

CT: Computed Tomography

DL: Deep Learning

DNR: Do Not Resuscitate

DWT: Discrete Wavelet Transform

F1: F1 Score

FLOPS: Floating Point Operations Per Second

GLCM: Gray Level Co-occurrence Matrix

HCPs: Healthcare Providers

HGG: High-Grade Glioma

ICH: Intracranial Hemorrhage

ICES: Intraoperative Stereotactic Computed Tomography-Guided Endoscopic Surgery

ILSVRC: ImageNet Large Scale Visual Recognition Challenge

IPH: Intraparenchymal Hemorrhage

LBP: Local Binary Patterns

LReLU: Leaky Rectified Linear Unit

LSTM: Long Short-Term Memory

mAP: Mean Average Precision

MBConv: Mobile Convolution

MISTIE: Minimally Invasive Surgery with Thrombolysis in Intracerebral Hemorrhage Evacuation

ML: Machine Learning

MRI: Magnetic Resonance Imaging

NCCT: Non-Contrast Computed Tomography

NN: Neural Network

NPV: Negative Predictive Value

PCA: Principal Component Analysis

PPV: Positive Predictive Value

PRES: Posterior Reversible Encephalopathy Syndrome

RCT: Randomized Controlled Trial

RCVS: Reversible Cerebral Vasoconstrictive Syndrome

ReLU: Rectified Linear Unit

ResNet: Residual Network

RF: Random Forest

RNN: Recurrent Neural Network

ROC: Receiver Operating Characteristics

ROI: Region of Interest

RSNA: Radiological Society of North America

SAH: Subarachnoid Hemorrhage

SE: Squeeze-and-Excitation

SVM: Support Vector Machine

VGGNet: Visual Geometry Group Network

CHAPTER I
Introduction

This chapter presents a brief background that includes medical information about intracranial hemorrhage, the role of CT technology in diagnosing intracranial hemorrhage, the evolution of intracranial hemorrhage detection and analysis systems, and an overview of the proposed AI-powered innovations for CT scan analysis.

Background

Intracranial hemorrhage is the collective term for accumulation of blood within the skull, most commonly from ruptured blood vessels. Early detection of hemorrhages is essential for their treatment. There are various categories of intracranial hemorrhages according to their location, such as epidural, subdural, subarachnoid and intraparenchymal types. They all have their individual information and structural imaging appearances, which can make the diagnosis challenging for each of them. Intracranial hemorrhages, unlike other medical conditions needed timely identification to avoid life-threatening situations like brain damaged or even death. In particular, new technology has made it clear that intracranial hemorrhage needs to be diagnosed via CT scans because they can detect subtle bleeds quickly and in a way that isn't practical when you are dealing with patients in an acute emergency (Piao al., 2023).

CT scanning - which enables quick, precise images of blood that has been scattered over the brain - is paramount in diagnosing each kind of cerebral hemorrhage. CT ANGIOGRAPHY: - It is performed by generating 3D X-rays of brain originating from different angles and later they are integrated to give detailed image Intracranial hemorrhages, for example, generally appear as regions of increased density or whiteness on a CT image because blood absorbs more X-rays than the brain tissue surrounding it (Chang et al., 2018). Doctors can more easily identify the extremity and volume of a hemorrhage along with its impact on surrounding tissues based on this degree of contrast between images. The key advantage of CT scanning is an automated process that breaks the complex task of infarct segmentation down to low-dimensional feature representations, and its subsequent use by a trained machine learning model for efficient stroke detection in real-time under emergency conditions. Moreover, the

CT is able to give differential diagnoses between all kinds of brain hemorrhage including subdural and epidural for appropriate treatment (Piao al., 2023).

The different sizes, shapes and locations of intracranial hemorrhages are challenges for estimating CT image. Knowing where and why an intracranial hemorrhage is happening is critical to providing timely care. Various AI-powered techniques have been proposed and realized including automated deep learning model-based foot print excavation (MacIntosh et al., 2023), fuzzy entropy cloning for accurate region identification (Meng et al., 2022). In addition to incorporating level set approaches with AI capabilities by (Gibson at el., 2022). AI algorithms have been taught to help detect and classify placement of hemorrhages in order to provide assistance for critical healthcare decisions. Although manual measurement analysis of CT images may result in human error, more advanced AI-based systems are required to improve diagnosis to accurately and quickly generate the parameters (Piao al., 2023).

With the rapid growth of artificial intelligence (AI) and deep learning, the analysis of CT images to detect intracranial hemorrhage (ICH) has had substantial progress. Diagnostic accuracy can be improved by using many methods including hybrid and deep learning approaches. For example, Mohammed et al. (2022) presented a multi-method diagnostic system by combining three pretrained CNNs, GoogLeNet, ResNet-50, and AlexNet, with SVM for feature extraction and classification, complemented by Principal Component Analysis (PCA) for dimensionality reduction. The subtle appearance of ICH in CT images is a difficulty that these systems seek to overcome. Additional studies prematurely encourage evolving CNN-based architectures in combination with other deep learning methods such as LSTM, while also adding GLCM features as has been done by Mucha and Babu (2024). Improving classification accuracy is important, as well, and helps mitigate training failures due to hematic pooling regions that may normally appear in the same volume as an actual intracranial hematoma. Sengupta et al. The use of bidirectional LSTM networks with genetic algorithms which are capable of improving detection in 3D scans was successfully presented by Zhang et al. (2023). Moreover, Yeo et al. Search for Net Anatomy: (2023): CNN-based applications outperformed necessity gen-based methods, analyzing CNN’s hierarchical structure as an important feature for optimizing deep learning algorithms by refining feature extraction processes. Cortés-

Ferre et al. (2023) reaffirm deep learning's future role in automating the detection of ICH, and that its performance is superior to that of manual and task-oriented approaches.

Detection and classification of intracranial hemorrhage (ICH) regions are key in order to distinguish between different types of hemorrhages, thus justifying further work in this domain. In this thesis, we introduced a system that employs deep learning models to effectively detect and classify ICH in computed tomography (CT) images. The study used deep pretrained models with transfer learning to improve performance for ICH detection. The system works with 2-D axial images from computed tomography (CT) scans in which it detects and segments hemorrhage areas. This not only improves the feature extraction but also can be used as a framework for future extraction. The proposed techniques enhance the accuracy of ICH detection by concentrating on the visual coherent regions in the input images, leading to better computer-aided diagnostic tools in future clinical implementations. Overall, this thesis demonstrates the promise of deep learning in the field of medical imaging, in particular with respect to the rapid and reliable diagnosis of critical illnesses such as intracranial hemorrhage.

The problem statement and limitations:

Intracranial hemorrhage (ICH) detection poses several challenges mainly owing to the intrinsic complexity of brain anatomy and the limitations of the generations of imaging methods available today. These problems may result in missed diagnoses, especially in high-pressure health-care environments. In the subsequent sections, we describe the main issues related to ICH detection. The potential adverse effects of ICH management are large, and due to the complexity of ICH these effects occur on all levels, diagnosis and treatment outcome. These give rise to its challenges are accurate prognostication, early care decisions and the challenges within the condition. Early care limitations like as effect of DNR "The DNR order informs healthcare providers not to perform CPR if a person's heart stops beating or their breathing stops": Early DNR orders are associated with approximately doubled hazard of death, with studies suggesting poor prognostication associated with them and subsequent mortality (Zahuranec et al., 2007).

Challenges in Detection and Classification:

Due to the fact that the manual diagnosis method is time-consuming and laborious, automatic ICH recognition and classification techniques from AI models are absolutely needed (Meng et al., 2022). Early diagnosis improves ICH scan scheduling and improves treatment. Therefore, numerous research studies are developing computer-aided diagnosis (CAD) for ICH segmentation. The CAD system based on (i) manual diagnosis where experts have to be present in order to provide accurate input (ii) automated diagnosis where hemorrhage has been diagnosed with no medical intervention (Kidwell et al., 2004). Recent advancements of computer vision methods, particularly deep learning (DL), have demonstrated great potential to learn meaningful representation from healthcare images (J. Ljungqvist et al., 2017).

Prognostic Challenges: Existing prognostic tools like the ICH Score suffer from biases and weaknesses in treatment decision-making (Chu & Hwang, 2016).

Perspectives: Subjective clinical judgments: Clinical assessments made by health care providers (HCPs) early on may not positively correlate with outcomes and affect decisions about critical care (Chu & Hwang, 2016).

Data Scarcity and Annotation Challenges: There is also a scarcity of labeled data for training Deep learning (DL) models, which greatly hinders the establishment of reliable detection algorithms (Sengupta et al., 2023). 3D CT images is resource-intensive, and inaccurate bounding boxes can negatively impact model performance (Sanner et al., 2024). Classification Accuracy for clinical applications, attaining high classification accuracy is paramount (Sengupta et al., 2023).

Treatment Complexity: This diversification means that ICH can occur from different etiologies, leading to diagnostic challenges and treatment versatility. Hypertension and cerebral amyloid angiopathy are among conditions that call for customized management strategies (Schaefer & Edjlali, 2024). Surgical Options: While surgical options exist, they are usually limited to the condition of the patient and the timing of the surgery, which may impact the overall prognosis (O’Carroll et al., 2021).

Time Constraints in Emergency Settings: Trauma cases require rapid assessment and treatment and there is often not enough time to review CT images in detail, which can result in missed hemorrhages. This dependence on clinical students and junior staff can worsen the situation since they may fail to notice subtle signs of ICH (Sanner et al., 2024).

Therefore, this thesis is conducted according to the following objectives:

- This is followed by the detection of Intracranial hemorrhage (ICH) regions and then enhancing these regions using proposed methods.
- Optimal success rates are achieved, in both single and combined datasets, for detection of areas related to Intracranial hemorrhage (ICH).
- Make deep learning architectures detection better by giving them clearer and more distinct hemorrhage regions to classify.

Thesis Layout

The thesis chapter 1 summaries the basics and layout of this thesis. Introduction In this second chapter, as literature review. The basics of Intracranial Hemorrhage (ICH) are introduced in Chapter 3. In chapter 4, the methodology of thesis is described. Subsequently in Chapter 5 the results and discussions are shown. Finally, conclusion is stated in chapter 6.

CHAPTER II

Literature Review

This chapter review the previous works and advancements related to deep learning-based intracranial hemorrhage detection. It outlines the used methods and datasets, as well as the evaluation result realized in prior work, summarizing progress and recognizing gaps to help guide future research.

Mohammed et al. (2022) proposed the multi-method diagnosis system in which identifies intracranial hemorrhages using CT images instantly. This system was decomposed into three different methods in classifying CT images reliably. To classify the dataset using deep learning techniques, initially the first system used three pretrained knowledge models in Convolutional Neural Networks (CNN), i.e., GoogLeNet, ResNet-50 and AlexNet. In our second system, we developed a hybrid technique by integrating these deep learning models with Support Vector Machine (SVM) for better feature extraction and classification accuracy. Third, the third system used an Artificial Neural Network (ANN) which included features learned by aforementioned deep learning models and dimensionality reduction was made as principal component analysis. Further, Gray Level Co-occurrence Matrix (GLCM) and Local Binary Patterns (LBP), a pair of patterns in the convolutional layer were extracted as features to enhance classification performance using ANN. As a dataset to demonstrate the capabilities of our proposed system, we used CT data obtained from Near East Hospital in Cyprus. The best ANN network considering the fusion with 18 deep features from AlexNet in GLCM and LBP, which achieved an accuracy of (0.993) precision of (0.9936), sensitivity was equal to %99.5, specificity was greater than percent (%99/57%), AUC (%98/84%).

Majeed et al. (2023) presented an approach to the identification and classification of intracranial hemorrhage (ICH) on CT images with ML methods. The study highlighted the critical role of early diagnosis for brain diseases, particularly ICH, and proposed a triage algorithm to promote rapid identification and treatment. A brief description of the proposed method: 4 Main steps Before any of the deep learning models could be trained, a preprocessing pipeline was created and used to remove bone from each skull in order to automatically segment out brain tissue within CT images. The second step involved performing feature extraction from CT to extract the pertinent features followed by preparing this data for further classification. Thirdly, we applied a right feature selection model which is Principal Component Analysis (PCA) to improve performance of models by reducing redundancy in features selected. The dataset was then grouped in non-normal and normal patterns following the standard procedure for classification with machine learning, such as Support vector machine (SVM), Random Forest (RF) and Decision Tree. Its accuracy in detection on Random Forest Model showed much higher value of 92.5 % that proved the effectiveness of detecting ICH by it. The machine learning models were trained and tested on a CT-scan dataset, but the specific details for the data set are not provided. This high accuracy of the Random Forest model (92.5 %) in detecting ICH relative to other methods used for this study.

Mucha et al. (2024) presented a hybrid approach to classify ICH in CT images employing both image-based GLCM features and deep learning methods, namely CNN and LSTM. This system was designed to automatically classify radiological data for ICH diagnosis, where CNN and LSTM units were combined using a logistic function. A large dataset consisting of 12,852 radiological reports was preprocessed first: it comprised 8,738 for training and another set to be used as validation (1,543) and testing. Afterward, the dataset was annotated by a grad student to produce ground-truth. In the first stage, preprocessing of input images was performed using Discrete Wavelet Transform (DWT) for feature extraction from image. Then the image-based features using GLCM was calculated like contrast, energy and homogeneity followed by subsequent feature vector generation from images Discrete Cosine Transform (DCT). In the last phase of this code, we tried to link back those result with how well our classifier was working on highly imbalanced dataset and for that purpose used ROC curve. The dataset that the study employed was comprised of 12,852 radiological reports; specifically, there were 10,966 negatives and approximately only ICH positive (1,886 cases in total). The performance assessment of the classifier included specific measures including Accuracy, Recall, and F1-score with ROC curve to ensure a holistic evaluation.

Yeo et al. (2023) To automatically detect intracranial hemorrhage (ICH) and its subtypes on non-contrast CT (NCCT) head studies, proposed a deep learning model

This was intentionally implemented as a system for benchmarking different preprocessing and model design to improve the detection accuracy. At first, the DL model was based on a Convolutional Neural Network (CNN) architecture and more specifically accessed to ResNet models pretrained on ImageNet. The regime was divided among three stages. The model was trained in stage one with a training dataset of 21,744 NCCT head studies—40.8% were positive for intracranial hemorrhage. We used the FORCE11 trust-sample of university emails, with test datasets from India which uses a different flow and training sets on multiple institutions across USA, Canada, Brazil. The second stage optimized model training using different techniques such as input image-windowed and concatenated inputs. Furthermore, a recurrent neural network (RNN) has been added after the CNN to discover interslice dependencies which improves overall performance of our model. Finally, the performance of our model in terms of metrics such as area under receiver operating characteristic curve (AUC-ROC) and micro averaged precision (mAP), was evaluated. This improved the performance a lot, and (mAP) increased from 0.77 to 0.93; AUC-ROCAUC-ROC rose from 0.854 to 0.966 At the balanced operating point, the model achieved an accuracy of between 0.86 to 0.96 that converted into further number correct classifications for test samples region. The model successfully identified cases of ICH and accurately discriminated negative from positive for all included studies while maintaining sensitivities that ranged between 0.87–1.00 and specificities ranging between 0.85–0.96 at an operating point with high-sensitivity capabilities. Evaluation of the system was conducted on a multi-center retrospective dataset and validated in an independent cohort to ensure robust performance across different populations. Once pre-processing techniques and the use of RNN framework were performed, this resulted in area under ROC curve (AUC-ROC) to be ≥0.949 for all classes, a significant improvement.

Cortés-Ferre et al. (2023) for detection concerning intracranial hemorrhages on CT images in human deep-learning based approach using EfficientNet, this shall support diagnostic decisions by clinicians. It was trained to classify CT scan slice for whether there is hemorrhage from scans. In the first stage, we trained models to predict whether or not small slices of CT scans contained hemorrhage using an accuracy of 92.7% and ROC AUC score 0.978 At the second stage, Grad-CAM method was applied to interpret this classification and highlighted in CT images where it focused on. It was also trained on a pre-processed version of the original Kaggle dataset, with classification labels transformed to binary format (ICH or not ICH). In the case of ICH detection, model performed well with a 92.7% accuracy and also gave attention via Grad-CAM which improves interpretability of decisions by deep learning models. Note that as of this point the model is for research use only -- we recommend technical expertise to run it effectively, while its positive diagnostic identification capability reached 92.3%, indicating high discriminative power for detecting ICH; it successfully identified a significant proportion of true-positive cases. Its specificity was 97.7%, indicating its excellent ability to avoid false positive predictions by correctly identifying patients without ICH

Thalhammer, M. et al. (2023) conducted a study exploring the benefits of deep learning-based artifact reduction in sparse-view cranial CT scans as well as their influence on automated hemorrhage detection. The system was separated into two fundamental methodologies. For artifact reduction in simulated sparse-view cranial CT scans of 3,000 patients with a public dataset, we initially trained a U-Net model. Subsequently, the EfficientNetB2 model was trained using CT full-view data of 17,545 patients for automatic hemorrhage detection. Detection performance was evaluated using the area under the receiver operator characteristic curve (AUC), with differences assessed through the DeLong test and confusion matrices. Before comparing with a TV postprocessing approach. Compared to no processing, both U-Net and TV postprocessing led to much higher image quality. Also in detection, U-Net postprocessing enabled achieving 0.97 AUC with only 512 (vs 4096) and even just at most half of these views (256; AUC:0.97), whereas number of hemorrhages detected was minimally reduced when compared across architectures The mean structural similarity index measure significantly increased compared with the unprocessed images, suggesting an improvement in image quality. The results were significant at a cluster-corrected significance threshold of 0.00017 adapted to Bonferroni-correction of multiple comparisons on voxel level (Tables S3, S4). In summary, we found that U-Net-based artifact reduction markedly improved automated hemorrhage detection in sparse-view cranial CTs and could possibly be beneficial for clinical use.

Nizarudeen, S. et al. (2022) developed ConceptionNet, a new automated algorithm for detection and classification of intracranial hemorrhage by means of deep learning techniques. It is built using modern transfer learning techniques where the base pre-trained model has been trained on ImageNet. More Initially, the algorithm used pre-trained networks (in this case Inception and EfficientNetB0) with fixed weights to process CT images. Subsequently, these models' last layers were fine-tuned on a hemorrhage dataset with an aim to correctly identify the most likely class of hemorrhage in the next stage. Next, the ConceptionNet was trained on this dataset as well to improve detection and classification. We trained a system on 2,848 CT images from 82 subjects (46 males and 36 females). The results of this study are an Area Under the Curve (AUC) assessment, evaluating algorithm performance for five hemorrhage types: Epidural (0.983), Intraparenchymal (1.0), Intraventricular (.968), Subarachnoid (1.0), and Subdural (1.0). The accuracy of the models was 0.96, for EfficientNetB0 and ConceptionNet it is 95% about from InceptionV3. The results prove that the algorithm was performed well and may have a place in aiding junior radiologists to diagnose intracranial hemorrhage. Although not to specific level of sensitivity and specificity, high overall performance must be implied since the AUC classification accuracy are good.

Sengupta et al. (2023) presented a method on 3D CT brain images to detect intracranial hemorrhage, but this research is targeted at the difficulties in collecting labeled data required for recognition. The approach has been divided into several key steps. Images used were first obtained from the image acquisition stage of RSNA 2019 dataset. Forward of this process, an Otsu's thresholding method was used for step 2 to get the region of interest (RoI) as follows. After segmentation, the region of interest (RoIs) regions was fused to convert into vectors using Tamura features (directionality; contrast and coarseness), local ternary pattern with gradient descriptor (GLTP descriptors). A reduction from the redundancy of the extracted vectors, due to their dimensionality is implemented in this model by a modified genetic algorithm with infinite feature selection technique which was used to enhance efficiency. The optimal vectors were then passed through a Bi-directional Long Short-Term Memory (Bi-LSTM) network to classify different subtypes of intracranial hemorrhage -subdural, intra-parenchymal, subarachnoid and epidural hemorrhages as well as intraventricular bleed. A dataset from the RSNA 2019 database provided required 3D CT brain images for analysis, and the system was tested using this specific data. Results: The modified genetic algorithm- Bi-LSTM method exhibited promising performance, with sensitivity 99.40%, accuracy 99.80% and specificity 99.48%. The weak results were overcome because the proposed method works better than classical machine learning models like Naïve Bayes, Random Forest and Support Vector Machine (SVM), Recurrent Neural Network (RNN) with LSTM networks.

Abrigo et al. (2023) The study developed an AI model for detecting acute ICH on CT scans, in which to evaluate the diagnostic performance of this model within clinical practice among a population from Hong Kong crisis healthcare system. We trained the model on a private dataset based on publicly available CT volumes of around 750,000 expert-labeled images. It predicts the ICH status associated with each CT scan and returns five potential ICH-positive slices for further evaluation. They validated the model in a retrospective database of 1372 unenhanced head CT scans from an institutional archive (84 ICH, 6.1% positive). The AUC of diagnostic performance with the model was 0.842 (95%, confidence interval, CI: 0.791-0.894; P<0.001). This model reached a sensitivity of 73%, specificity of 79% and showed an accuracy, positive predictive value & negative prediction rate was: > The model detected 62 true positive scans with that of 22 false-negative scans. If the slices chosen by 10 different users are reintroduced into model evaluation, this could translate to as few as six false negatives. These findings underscore the potential utility of this model as an adjunct in clinical settings to identify ICH, although additional adjustments may be necessary to increase sensitivity and decrease false negatives.

Agrawal et al. (2023) Based on deep learning techniques, with attention to convolutional neural networks (CNN), Hagerty et al., Further investigated the automatic identification of intracranial hemorrhage (ICH) using head CT images in his performed study. The analysis comprised of a few stages: First, literature about detection of ICH in head CT with automatic methods was searched. In the following phase, the effectiveness of AI algorithms in ranking radiology worklists to decrease ICH triage time was assessed. Additionally, the study determined AI algorithms to be capable of identifying small ICH that may go unseen by radiologists. This comparison demonstrates the efficiency of different CNN-based deep learning methods in detecting ICH. While detailed lists of datasets used in each study are not provided within this context, the review identified 15 studies that develop and validate algorithms using head CT scans. They conclude that AI algorithms can greatly improve the ICH detection efficiency, which may potentially result in better clinical outcomes.

Rashid, M. H. O et al. (2023) An automated deep learning-based method for the detection of ICH from CT images in this study. This is a step-by-step procedure, first of all the data were prepared and I trained one image model from large data set patient CT scans. This includes preprocessing such as normalization, windowing and augmentation to improve the quality of images. To fine-tune the model during training, 30% of train data was left for validation. The research used the Radiological Society of North America's (RSNA) dataset, with 752803 training images and 121232 test images. This large dataset is important for learning a model generalized enough to be reliable with new data. The accuracy of proposed model is able to classify ICH in test data with an astonishing 98%. Sensitivity and specificity are not available but higher accuracy suggest better ability to diagnose ICH.

Ozsahin et al. (2021) in this study was made of the mechanism from the application of Deep Convolutional Neural Network (DCNN), to classify people with Alzheimer's Disease (AD), Mild Cognitive Impairment (MCI) and Cognitively Normal (CN) by tau protein Positron Emission Tomography (PET) images. The Alzheimer's Disease Neuroimaging Initiative (ADNI) database, which included around 40,000 2-dimensional images from 1097 baseline and follow-up tau positron emission tomography (PET) scans (AV-1451), consisting of 86 Alzheimer's Disease (AD), 442 mild cognitive impairment (MCI) and 569 cognitively normal (CN) subjects. The processing was standardized, and image enhancement techniques such as sharpening and contrast adjustment were performed in order to minimize variations due to different imaging devices. Then, two deep convolutional neural network (CNN) models were utilized; the first included two convolutional and two dense layers, while the second included three convolutional and three dense layers.In binary classification experiments (AD vs. CN, MCI vs. CN), Receiver Operating Characteristics Area Under the Curve (ROC AUC) scores were 0.9943 and 0.9908, respectively. For the three-class classification experiments (AD vs. MCI vs. CN), the convolutional neural networks reached a macro-averaged F1 score of 0.9827, reflecting high concordance rate across the three categories. The findings of this study suggest that deep convolutional neural network architecture is an efficient method for classifying AD, MCI, and CN subjects based on tau PET images alone.

Sekeroglu, B. et al. (2021) proposed A hybrid model combining Support Vector Regression (SVR) and Emotional Artificial Neural Networks (EANNs) for body fat percentage (BFP) predictive modeling with good accuracy. It aimed to outline this common data restriction in BFP where new data dominates, even though we are not aware of this from the state of knowledge (traditional BFP estimation methods). The model was trained, with eight important features/attributes per individual from a dataset consisting of 2000 such people and showed excellent predictive performance in the return metrics: $R^2 = 0.991$, RMSE = 0.0125, and rRMSE = 3.15%, outperforming seven other baseline models (decision trees, random forest, and XGBoost, among them). The strongest predictor was abdominal circumference, while age was a weak factor. To the best of our knowledge, the SVR-EANN model represents the first new prediction model for predicting BFP to improve obesity management programs on a large-scale survey of data.

Chapter III

Intracranial Hemorrhage (ICH)

This chapter presents an overview of the intracranial hemorrhage disease, The types, Causes and risk factors, Diagnostic Techniques, Symptoms and Clinical Presentation

Intracranial Hemorrhage (ICH) review:

The disease of intracranial hemorrhage occurring in the brain due to the blood vessel leaking which causes inactive body functions such as memory loss, speech, and eyesight (Li et al., 2022). The most significant risk factors in intracranial hemorrhages are infected blood vessel walls and leakages in the vein (Remedios et al., 2020). CT imaging is the preferred modality in intracranial hemorrhage detection as compared to other imaging modalities owing to its low cost, high sensitivity, speed, and wide availability (Kuo et al., 2019). The lesions of intracranial hemorrhage are brightly defined in the CT imaging modality. Intracranial hemorrhage lesions are manually detected based on the CT scan, which is difficult due to artifacts in the CT scan, uneven boundaries, noise, and overlapping pixel intensities (Karki et al., 2020), (Duperron et al., 2019). Thus, the manual delineation is subjected to the intra-observer and inter-observer, and it relies heavily on the physician's know-how (Sengupta et al., 2022). Bleeding types have different severity degrees and interventions (Ye et al., 2019). Intraparenchymal hemorrhage (IPH) Subdural hemorrhage represents around 15% of all strokes (Sacco et al., 2009). The predominant causes in older individuals are elevated blood pressure, cerebrovascular amyloid angiopathy, anticoagulation, hemorrhagic transformation of acute ischemic strokes, and primary or secondary malignancies, contingent upon their size and location. Common vascular abnormalities, including arteriovenous malformations, cavernous malformations, cerebral venous sinus thrombosis, as well as uncommon conditions like moyamoya and dural arteriovenous fistulas, should be contemplated in younger individuals and children. Infrequent etiologies of IPH including Reversible Cerebral Vasoconstrictive Syndrome (RCVS), posterior reversible encephalopathy syndrome (PRES), vasculitis, pharmacological toxicity, and infections including mucormycosis and aspergillosis.

inflammation and permeability of the blood brain barrier (Fischbein et al., 2010). Given that subdural and epidural hemorrhages are typically associated with head trauma, it is crucial to provide a history of head injury. Nonetheless, spontaneous hemorrhages may occur even in individuals on anticoagulant or antiplatelet treatment. Additionally observed in patients with coagulopathies, dural and osteodural arteriovenous fistulas, cerebral hypotension, and dural or calvarial metastases (Fischbein et al., 2010). Subarachnoid hemorrhage (SAH) ranks as the third most common subtype of stroke. A fall in the incidence of SAH has been reported over the previous few decades possibly due to lifestyle influences, the cessation of smoking and improved control of hypertension. Approximately one in four patients with SAH doesn't live long enough to be admitted to the hospital. But those who reach the hospital tend to have better outcomes, though they remain at elevated risk for long-term neuropsychiatric problems such as depression. With the average age of onset around mid-50 s, this condition still has a tremendous public health burden, as patients suffer downstream for many years (Claassen et al., 2022). Subarachnoid hemorrhage (SAH) is defined by the presence of blood in the cerebrospinal fluid (CSF) between the basal cisterns and subarachnoid spaces of the cerebral hemispheres, situated between the arachnoid mater and pia mater. The yearly occurrence of nontraumatic subarachnoid hemorrhage (SAH) is 9 per 100,000 persons. This rare yet critical occurrence has an estimated fatality rate of 40% within the initial 48 hours and is associated with the rupture of an intracranial aneurysm in 85% of instances (Fischbein et al., 2010). Hypertensive Hemorrhage Chronic, inadequately managed hypertension is a prevalent cause of cerebral bleeding. These individuals have a distinctive hypertensive vasculopathy characterized by lip hyalinosis of small- and medium-caliber vessels, including the lenticulostriate, thalamoperforating, pontine perforating arteries, and cerebellar arterioles. The rebleed rate from microaneurysms is 2% annually, with hemorrhages predominantly occurring in the basal ganglia (35–40%), thalami (10–20%), pons (5–10%), and cerebellum (5–10%) (Kranz et al.,218). And literally, hemorrhages are sometimes seen at the subcortical white matter (1–2%) Symptoms present differently based on the location of the hemorrhage. Microhemorrhage and lacunar infarction in the deep gray nuclei, brainstem, and cerebellum, together with generalized leukoaraiosis, corroborate the diagnosis (Fischbein et al., 2010). A little presence of blood product is noted in the occipital horns, without actual intraventricular hemorrhage. Patients usually have stable clinical conditions and clear consciousness (Fischbein et al., 2010). As Figure 1. Showes the different types of hemorrhages and their corresponding location within the skull (Li, Y. et al., 2012).

	Intraparenchymal	Intraventricular	Subarachnoid	Subdural	Epidural
Location	Inside of the brain	Inside of the ventricle	Between the arachnoid and the pia mater	Between the Dura and the arachnoid	Between the dura and the skull
Imaging	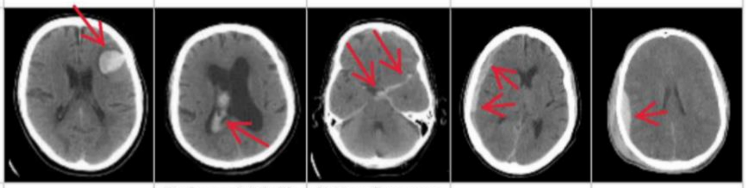				
Mechanism	High blood pressure, trauma, arteriovenous malformation, tumor, etc	Can be associated with both intraparenchymal and subarachnoid hemorrhages	Rupture of aneurysms or arteriovenous malformations or trauma	Trauma	Trauma or after surgery
Source	Arterial or venous	Arterial or venous	Predominantly arterial	Venous (bridging veins)	Arterial
Shape	Typically rounded	Conforms to ventricular shape	Tracks along the sulci and fissures	Crescent	Lentiform
Presentation	Acute (sudden onset of headache, nausea, vomiting)	Acute (sudden onset of headache, nausea, vomiting)	Acute (worst headache of life)	May be insidious (worsening headache)	Acute (skull fracture and altered mental status)

Fig. 1. Different types of hemorrhages and their corresponding location within the skull (Li, Y. et al., 2012)

Complexity of Hemorrhage Subtypes

Detection is challenging due to the wide variety of morphology of hemorrhagic lesions; these different subtypes (e.g., subdural, epidural) exhibit varying characteristic. There are more sophisticated models including those with deep learning that showed promise but were still not sufficient enough for accurately localizing and classifying these subtypes (Cheng et al., 2023). Nevertheless, the ongoing improvements in deep learning and automated detection methodologies are enhancing diagnostic precision and efficiency and have the potential to transform the standard of ICH management in clinical practice.

Causes and Risk Factors and Prediction Scores:

Common etiologies of spontaneous intracranial bleeding encompass injuries: incidents resulting in significant trauma to the cranium. Vascular disorders, intracranial arteriovenous malformations, dural arteriovenous fistulas, vein sinuses thrombus, cavernous malformations, hemorrhagic conversion of ischemic infarction, coagulopathy, and underlying cancers (Fischbein et al., 2010). Several clinical, laboratory, and radiographic factors that correlate with the risk of ICH following alteplase have surfaced. The strength of evidence for these associations varies, with some evidence consistently observed in large studies and other associations only observed in small, single-center cohort studies. Older age, more severe stroke, a higher initial glucose level, hypertension, congestive heart failure, renal impairment, diabetes mellitus, ischemic heart disease, atrial fibrillation, baseline antiplatelet use, leukoaraiosis, and visible acute infarct on brain imaging were all associated with increased risk of ICH in a systematic review and metanalysis of 55 studies but current smoking was associated with reduced risk (Whiteley et al., 2012). Also, the authors showed a signal for a statin use and ICH in this meta-analysis based on a few subjects that could, however, not be confirmed in a follow up study of >20 000 patients (Messé SR et al., 2013). In this meta-analysis time from symptom onset to alteplase was not associated with ICH risk, consistent with other studies (Emberson et al., 2014), (Whiteley WN et al., 2016). Microhemorrhages on pretreatment magnetic resonance imaging have also been associated with a higher risk of ICH after alteplase, although the absolute increase in risk is modest (Charidimou A et al., 2015). The comprehensive nature of many ICH risk factors means that they are often highly interrelated, which complicates the estimation of the independent additive risk of each factor, particularly in small studies with insufficient power to perform comprehensive multivariable analyses. Atrial fibrillation, warfarin use (independent of prothrombin time), age and clinical stroke severity have all been associated with increased risk of ICH, but each is usually correlated with the other variables (Kimura et al., 2005). Moreover, the increase in absolute risk of ICH conferred by each of these factors also widely differs, which is an essential consideration in evaluating their clinical significance (Yaghi et al., 2017). Thrombolytic therapy induced hemorrhage can be the result of breakdown of the blood-brain barrier and reperfusion of damaged cerebral tissue (Chen et al., 2023).

Symptoms and Clinical Presentation:

The four most frequent symptoms of the disease are decreased consciousness level (47.5%), headache (38.1%), coma (9%), and seizure (5.4%). The initial diagnosis of patients with reduced level of consciousness was lobar (54%) and putamen hemorrhage (30.4%) in most cases (Bahrami et al., 2022). Symptom severity may increase during the initial 24–72 h after onset, requiring immediate emergency department evaluation (Lee et al.,2018). There is regional variation in the clinical features, but signs of increased intracranial pressure are commonly detected, resulting from the mass effect of the hematoma (Carhuapoma et al., 2009).

Diagnostic Techniques:

Intracerebral hemorrhage is often diagnosed via imaging modalities such as brain computed tomography (CT), magnetic resonance imaging (MRI), as well as blood tests, coagulation profiles, and angiography (CT, MRI, or selective). These techniques can elucidate the etiology and evaluate the risk of rebleeding (Anusha Bai et al., 2023). Traditional diagnostic methods are time-consuming and require high level of expertise and training, but deep learning techniques such as convolutional neural networks, transfer learning and others can analyze such datasets for efficient and effective diagnosis (Kulesh et al., 2020). In the treatment of intracerebral hemorrhage, minimally invasive surgery, including procedures such as MISTIE and neuroendoscopic surgery, is preferred. With early treatment and advanced devices like Apollo and Artemis™ that improve hematoma evacuation, the outcomes may be potentially improved. Emerging minimally invasive devices. (A) NICO BrainPath system and myriad handpiece (NICO Corp, Indianapolis, IN, USA). (B) The Apollo system. The Wand and aspiration–irrigation system (Penumbra Inc. Alameda, CA, USA). (C) Artemis Neuro Evacuation Device and Pump MAXTM aspiration system (Penumbra, Alameda, CA, USA) (Kobata et al., 2021). Endoscopic surgery Neuroendoscopic surgery allows for direct visualization of the area of ICH and removal via a less invasive approach than traditional craniotomy. Unlike the stereotactic procedure, it is also possible to achieve hemostasis at the bleeding point. ICES (Intraoperative Stereotactic Computed Tomography-Guided Endoscopic Surgery), a multicenter RCT, revealed substantial safety and efficacy (Vespa P et al., 2016). Stem cells can reproduce unlimited and can be matured into specialized function cells. Based on their differentiation capacity, they are classified into totipotent, pluripotent, and multipotent stem cells (Gage et al., 2000), (Jaenisch R et al., 2008). However, with the mobilization of regenerative medicine, more and more researchers have paid attention to stem cell and exosome therapy, which as a new method for the treatment of intracerebral hemorrhage, because of their potential intrinsic neuroprotection and neurores-toration. The regenerative, differentiation or secretory effects of stem cells can participate in the treatment of intracerebral hemorrhage directly or indirectly according to many animal studies (Zhou et al., 2022).

CHAPTER IV
Deep learning

This chapter explores deep learning principles, focusing on convolutional neural networks (CNNs) and their architectures, including LeNet, AlexNet, and ResNet. Key components, applications in image processing.

Deep learning

A subset of machine learning and consists of neural networks with multiple levels of abstraction to learn representations of data, particularly images. Deep Convolutional Neural Networks (DCNN): Used for image classification, image enhancement, and denoising) Automatically learn hierarchies of patterns from large datasets. CNNs are a cornerstone of using the principles behind deep learning to solve high-performance problems such as image processing, contributing to advances in fields such as medical imaging, autonomous driving, and game development. (Hsieh et al., 2024). Deep learning enables these computational models consisting of multiple processing layers to learn representations of data with many levels of abstraction. These approaches have dramatically improved in state-of-the-art performance in, among other things, speech recognition, visual object recognition, object detection, and a wide range of other fields such as drug discovery and genomics. Deep learning discovers complex structure in massive data sets, by applying the backpropagation algorithm to indicate how the machine should adjust its inner parameters, which are used to calculate the representation in each layer from the representation in the prior layer. Deep convolutional nets have delivered breakthroughs for processing images, video, speech, and audio while recurrent nets have revealed the power of deep learning for sequential data such as text and speech. (LeCun et al., 2015). Since the emergence of deep learning (DL), researchers have developed various convolutional neural network-based models that classify and analyze medical images including cancer, tuberculosis, and diagnostic radiological images. A Convolutional Neural Network (or CNN) is a kind of ANN that utilizes a multi-layer perceptron, where every neuron from one layer has links to all the neurons in the subsequent layer. CNN. They are networks, which apply the series of mathematical operations “Convolution. A number of neural network architectures being developed.

The regression, classification and denoising of images has been better in certain architectures than others. To train NNs, a backpropagation algorithm adjusts the weight contained in the NNs structure according to the data pattern while optimizing the error between predicted output and actual output (Simonyan et al., 2014), (He et al., 2016). That being said, convolutional neural networks are very similar to the traditional neural network, which can be considered as a neuron mapping which produces a graph that is acyclic. the sole distinction between this and a neural network is characterized by a neuron in a buried layer being linked only to a subset of the neurons in the preceding layer. This limited connectivity gives a potential good signal for the implicit learning of features. It is able to extract features on various levels due to the deep structure of the network. The filters learnt in the first layer may be interpreted as boundaries or masses of colors, the secondary layer can learn simple forms, the filtration of the consequent layers can learn parts of objects and finally, the last layers can recognize the whole objects (Aloysius et al. 2017).

Key Components of Deep Learning Architectures:

A. Convolutional Layer

Convolutional layer serves as the fundamental component of a ConvNet, where the majority of computations occur. This is a compilation of feature maps including neurons. The layer parameters are a number of trainable filters or kernels. These filters are convolved with the feature maps, generating a unique 2-dimensional activation map, grouping that only imagining the groups together along the depth dimension produces the output volume. 1D CNN On each feature map, neurons that lies at the same position in the kernel share the weight (parameter sharing) thereby decreasing the complexity of network by keeping number of parameters low (G.E. Hinton et al., 2012). The hyperparameter that regulates the degree of sparse connection within neurons in the two layers is referred to as the receptive field. The hyperparameters that dictate the dimensions of the output volume include depth (the number of filters in a layer), stride (the movement of the filter), and no padding (to manage the spatial dimensions of the output). Backpropagation used to train ConvNets The forward pass is convolution operation and the reverse pass is likewise a convolution but the filters are spatially flipped. Figure 2. illustrates core easier exercise of convent..

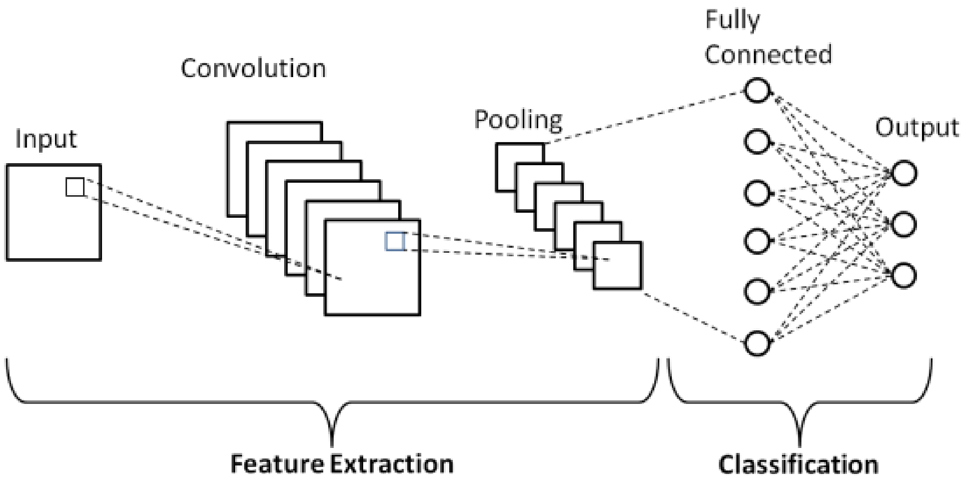

Fig. 2. A schematic structure for an elementary convolutional neural network (CNN) (Phung et al., 2018).

B. Pooling Layer

The Basic ConvNet architecture alternate with pooling layer and the pooling layer serve to reduce the spatial dimension of the activation maps (without losing information) as well as the number of parameters present in the net and thus decrease the computational complexity. This helps in controlling the overfitting issue. Max, average, stochastic pooling (M. D. Zeiler et al., 2013), spectral pooling (O. Rippel et al., 2015), spatial pyramid pooling (Nguyen A et al., 2015) and multiscale orderless pooling (Gong, Y et al., 2014) are some of the popular pooling functions. Figure 3. demonstrates the operation of max pooling (Minfei et al., 2022). Lastly, the work of (Alexey Dosovitskiy et al., 2015), inquiries about the necessity of a lot of ConvNet components and Demonstrated that max pooling layers may be substituted with convolutional layers featuring a stride of two. This is just meant for the basic networks that have demonstrated superior performance. a large amount of the evaluated complex architectures.

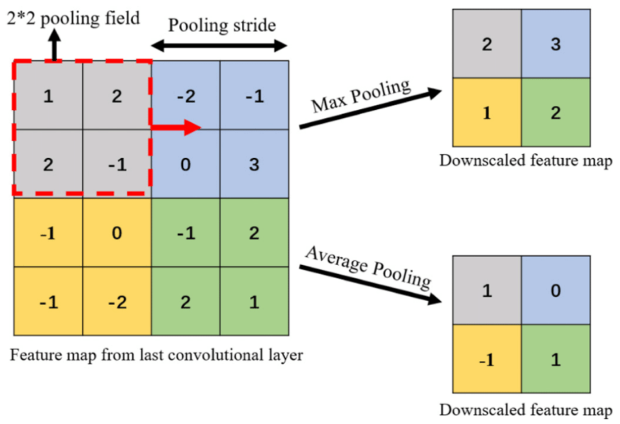

Fig. 3. Max and average pooling layer (Minfei et al., 2022).

C. Fully Connected Layer

In a conventional Neural Network, each neuron in this layer is entirely linked to every neuron in the preceding layer. This is the locus of high-level thinking. As the neurons are no longer organized spatially (1D), there is no way of telling if a convolutional layer is applied after the fully connected layer. As for example, "Network in Network" (NIN) developed by Zeiler et al. (2014) can replace the fully connected layer with the global average pooling Figure 4.

$$f(x) = max(0, x)$$

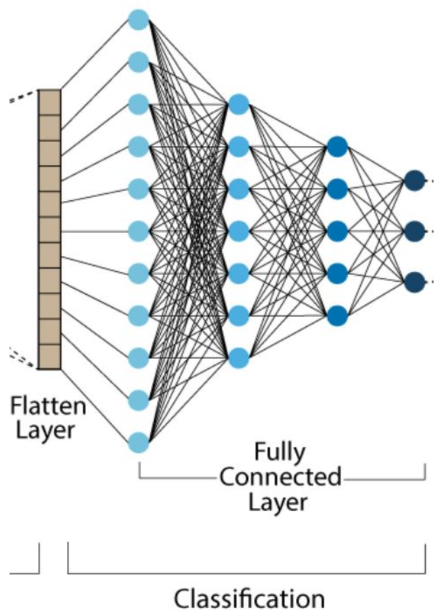

Fig.4. Fully connected layer (Rguibi et al., 2022).

D. Loss Layer

It is used for calculating loss or error (which is an penalty for the difference between expected output and actual output) in the loss layer, which is the last fully connected layer. SoftMax loss is used to predict a single class from K number of mutually exclusive classes. This is the most widely used loss function. In effect, it is multinomial logistic regression. It uses those predictions and makes them normal and feeds into a non-negative value function to produce a class probability distribution. It is a margin based classifier, Support Vector Machine is trained using Hinge loss. Using Euclidean loss allows for regression to real-valued labels (Aloysius et al., 2017).

Common CNN Archıtectures:

A. LeNet

LeCun et al. created one of the first Convolutional Neural Networks. In 1990 (LeCun. et al., 1990) and improved it later in 1998 (Y. LeCun et al., 1998). In this work Handwritten Digit Recognition task was solved using ConvNets. It is used for reading zip codes, digits, etc. At that time, there were not many high computing machines available, thus suspending the used of CNN.

B. AlexNet

It is the first work in Convolutional Networks with a significant impact and was widely used in the Computer Vision domain The Convolutional Network that was the first research done and was widely used in the Computer Vision domain was proposed in (Alex Krizhevsky et al., 2012) by Alex Krizhevsky, Ilya Sutskever, and Geoffrey Hinton. AlexNet, on the other hand, stacked all the convolutional layers on top of each other instead of interleaving convolutional and pooling layers like in LeNet. This network is also larger and more complex than LeNet. AlexNet won the ILSVRC-2012 competitions achieving the lowest top-1 and top-5 error rates on test data.

C. GoogleNet

Szegedy et al. reported that this ConvNet architecture was the winning architecture in the ILSVRC 2014 competition. (2014) from Google. They also recently introduced new Inception (v1) architecture allows for much better usage of the processing power in the various regions of the network. One realization of Inception module is GoogleNet with 22 layers and lower number of parameters than AlexNet Improvements to Inception-v1 eventually culminated in the introduction of Inception-v2 by (Ioffe et al., 2015), when it used more handwritten notes (among other things). We refer to this architecture as Inception-v3 (C. Szegedy et al., 2016) and introduced further refinements to it.

D. VGGNet

Karen Simonyan and Andrew Zisserman conducted an experiment that very carefully analyze the depth effect of a ConvNet with all other parameters held constant. It seems that this try has a huge number of parameters in the network however it was sagaciously overseen by applying very small 3X3 convolution filters on all layers. This work culminated in a new, more accurate ConvNet architecture, VGGNet. It had achieved second-place (Aloysius et al., 2017) in the ImageNet Large Scale Visual Recognition Challenge ILSVRC 2014.

E. Inception V4

Szegedy et al. later outlined a model that came out on top of GoogLeNet in 2017. This archicture utilizing Inception modules (Szegedy et al. 2014) with residual connections (G.E. Hinton et al. 2012). In 2015, it passed the ILSVRC (IMAGENET) Challenge with flying colors and won the competition as well.

F. EfficientNet

EfficientNet includes models ranging from B0 to B7, which can be used in image classification, object detection, segmentation, etc. Hence, EfficientNet is an important resource for deep learning practitioners (Tan et al., 2019). These components were all encapsulated in a baseline network depicted in Figure 5., specified as EfficientNet-B0, and a collection of scaled variants, Appendix F hereafter to use EfficientNet-B1, B2, B3, etc. in increments of φ with increasing can set depth, width, and resolution as a single coefficient. In general, this is achieved through adding layers, channels and more resolution to the input data (Tan et al., 2007).

Fig.5. EfficientNet base architecture (Singh et al., 2024)

G. DenseNet

A suggested CNN design exhibits a notable connectivity pattern: Each layer is entirely interconnected with all other layers inside a thick block, as seen in Figure 6. In this scenario, every layer has access to the feature maps of all preceding levels, facilitating extensive feature reutilization. This enables the model to be more compact and exhibit reduced overfitting. Furthermore, the bypass connections may be seen as offering the individual layers direct oversight from the loss function, so facilitating implicit deep supervision. The advantageous characteristics of DenseNet render it a suitable choice for per-pixel prediction tasks. A simultaneous study achieved state-of-the-art performance in semantic segmentation utilizing DenseNet, without pretraining or supplementary post-processing (Gao Huang et al., 2016) (Jégou, S. et al., 2015).

Traditional CNNs, like FlowNetS, compute the output of the l^{th} layer by passing a nonlinear transformation H over the output of the previous layer x_{l-1},

$$x_l = H_l(x_{l-1})$$

The spatial invariance of the network result is realized through cascading convolution and pooling, while the top layers obtain coarse semantic features. But with the very top of the network, detailed image information tends to get disappear.

To facilitate information flow between layers, DenseNet (Gao Huang et al., 2016) offers a simple connectivity pattern: the l^{th} layer receives the feature maps of all preceding layers as inputs:

$$x_l = H_l([x_0, x_1, \ldots, x_{l-1}])$$

where $[x_0, x_1, \ldots, x_{l-1}]$ is a single tensor formed by concatenation of output feature maps from preceding layers. This way, even the last layer can have access to the first layer input information. And every layer is directly supervised by the loss function through the shortcut connections. The $H_l(\cdot)$ is a composite function of four operations in consecutive order, batch normalization (BN), leaky rectified linear units (LReLU), a 3×3 convolution, and dropout. We call this composite function a layer.

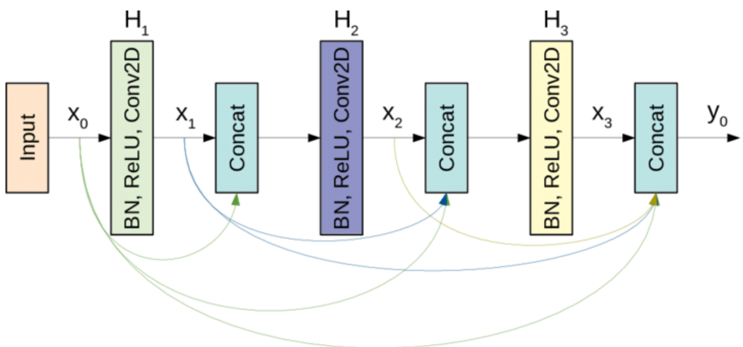

Fig.6. block used in the DenseNet architecture (Alshazly et al., 2021).

H. ResNet

ResNet is a common convolutional neural network that researchers have used in recent years to address computer vision tasks. This module prevents gradient vanishing caused by increasing the depth of the networks through the introduction of incomplete modules, and it avoids redundancy in data while providing high accuracy. It is simple and practical. Block ResNet operation is illustrated in Figure 7.(Alzubaidi et al., 2021). (K. He et al., 2015) introduced a residual learning framework. (2015), in which the layers learn residual functions concerning the input of the layers rather than unreferenced functions. They showed that their work specifically is important to train deeper networks because residual networks are easier to optimize and achieve much higher accuracy. The only drawback of this network is that it is quite costly to evaluate because of the high number of parameters. However, we could have limited the number of parameters to some degree without affecting the performance significantly, by eliminating the first Fully-Connected layer (most of the params are due to this layer).

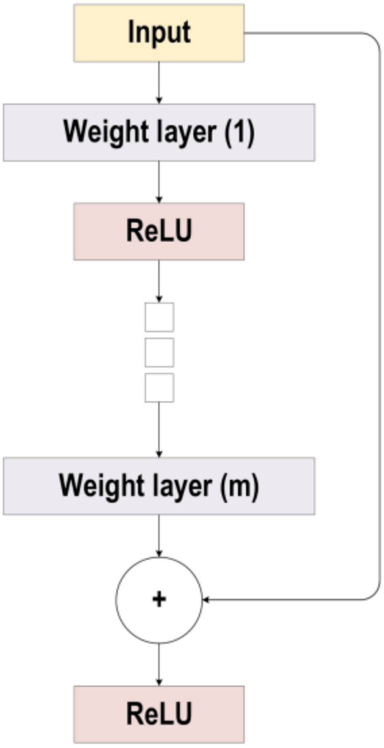

Fig.7. The block diagram for ResNet (Alzubaidi et al., 2021)

CHAPTER V
Methodology

Chapter outlines the methodology of the thesis. Methodology is divided into two sections. In the first part, we describe our proposed system in detail. In section two, are illustrated the performance measures used to evaluate the performance of the proposed system.

Materials and Methods

Dataset

In this thesis, we considered the Computed Tomography Images for Intracranial Hemorrhage Detection dataset (Hssayeni, M. et al., 2019). The dataset consists of 2500 brain and bone window head CT images for 82 patients. The brain images are used to detect the ICH using pretrained models. The total number of images for positive cases is 318, while the number of negative images is 2,183. Figure 8 presents the sample images for positive and negative cases.

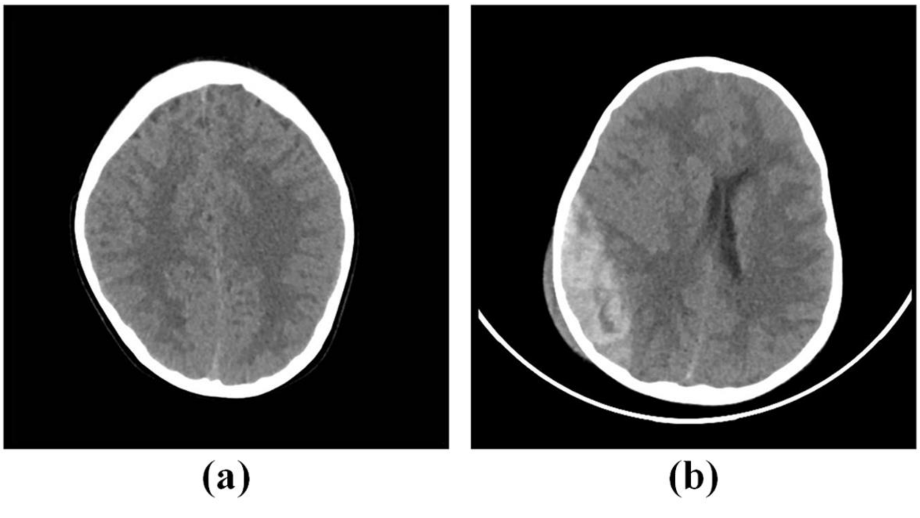

Fig. 8. Example images of the dataset (a) Normal and (b) ICH image.

Pretrained Models

This section presents brief information about the considered pretrained models.

EfficientNetB0

The baseline model provided in the EfficientNet (Tan et al., 2019) series, EfficientnetB0, features a core structure of MBConv blocks with integrated SE (Squeeze-and-Excitation) modules for improved accuracy. Figur 9 presents thearchitecture of EfficientNetB0 (Barman et al., 2024). The effectiveness of SE-based models was demonstrated in different types and combinations (based on re-positioning or not) of SE modules that were adjusted concerning a base architecture configuration, training them onto the ImageNet dataset. The EfficientNetB0 model is well-known for its robust and effective design, which has achieved state-of-the-art accuracy on the ImageNet dataset with 66 million parameters at only nearly 37 billion FLOPS. It is up to 8.4× more compact and 6.1x faster in making predictions than leading CNNs.

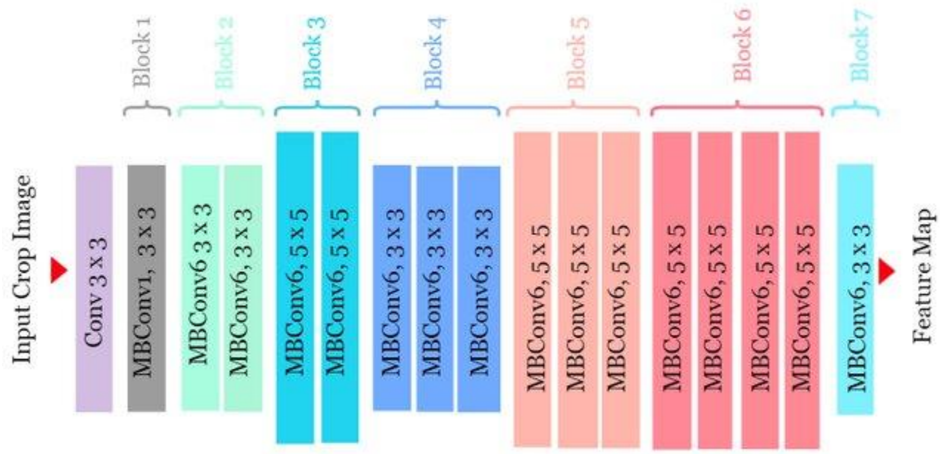

Fig. 9. EfficientNetB0 model architecture (Barman et al., 2024).

ResNet101

The models on top of CNNs, such as ResNet101 (He et al., 2016), consist of 101 convolutional layers and utilize residual connections within the design to make it effortless for information to get transmitted or passed from one layer to another without getting attenuated/vanishing during training. With the help of this depth and residual connections, the ResNet101 achieved 77.37% accuracy on the ImageNet dataset, making it an effective model for image classification tasks. Besides, its parameterization process is efficient, which makes it beneficial in different use cases . The typical architecture ofthe ResNet101 is summarised in Figure 10. (Kalshetty et al., 2023).

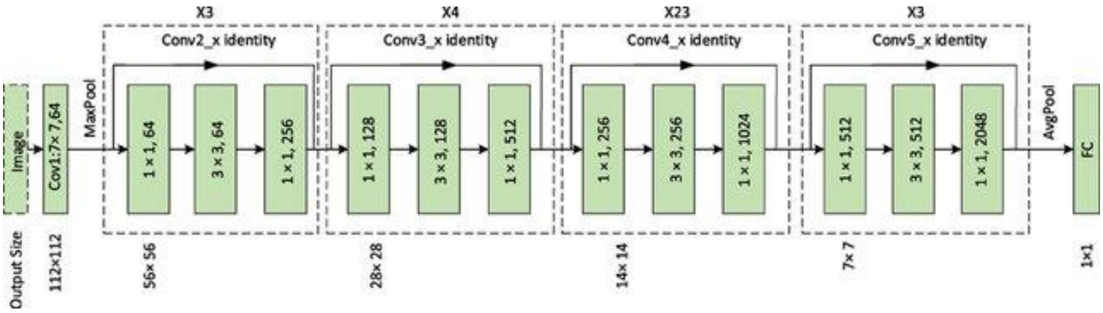

Fig. 10. Resnet101 model architecture (Kalshetty et al., 2023).

DenseNet201

The DenseNet201 (Huang et al., 2017) model has dense connections between layers for efficient information flow, and the high parameter usage helps to avoid gradient vanishing. It addresses the vanishing gradient problem by adding convolutional layers, pooling, batch normalization, ReLU, transition layers, and a classification layer as showen in figuer 11. (Kumar et al., 2021). This is a part of the DenseNet201, which provides flexibility and scalability to learn complex patterns in image classification tasks, with fewer computational resources reaching high performance without overfitting the ImageNet dataset.

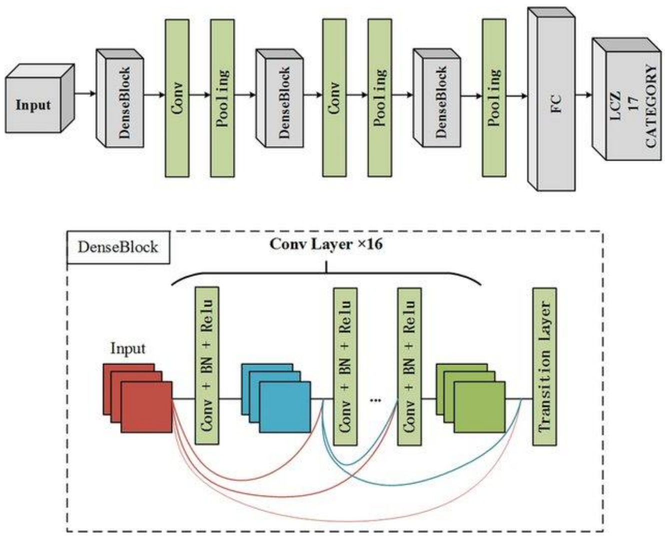

Fig. 11. DenseNet201 model architecture (Kumar et al., 2021)

Experimental Design

The experiments are performed using 5-fold cross-validation, and each model is trained for 100 epochs using the ImageNet weights to provide transfer learning. The batch size is set to 32, and the Adam Optimized is used with a fixed learning rate 1×10^{-4}. Even though the dataset is imbalanced and the number of positive cases is low, an augmentation is not applied to analyze the actual performances of the models. The mean of the fold results are calculated to assess the model performances. Figure 12. shows the block diagram of the experiments performed in this thesis.

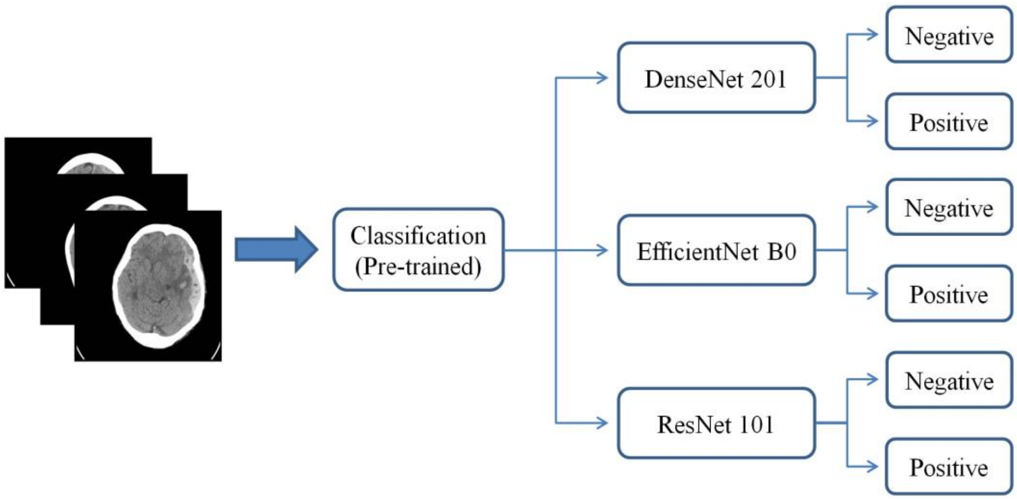

Fig. 12. Block diagram of the experiments.

Since the dataset is strongly imbalanced, we considered seven evaluation metrics to analyze the results. We used the accuracy metric to analyze the general detection ability of the models; however, due to the limitations of the accuracy metric in assessing the imbalanced data, we also considered the F1 score and Receiver Operating Characteristics (ROC) Area Under the Curve (AUC) for consistent analysis. Equations 1 and 2 show the formulae for the accuracy and F1 score.

Accuracy

It is an important metric to evaluate classification model performance. This equation shows that true positives (TP) and true negatives (TN) are significant in identifying the overall effectiveness of a model, false positives (FP), and false negatives (FN) also play a role. It is mathematically defined in Equation (1).

Where,

True Positives (TP): Instances correctly identified as positive.
True Negatives (TN): Instances correctly identified as negative.
False Positives (FP): Instances incorrectly identified as positive.
False Negatives (FN): Instances incorrectly identified as negative.

$$Accuracy = \frac{TP+TN}{TP+TN+FP+FN} \tag{1}$$

F1-Score

It is the harmonic mean or the weighted average of precision and recall. It is, by definition, a measure of a test's accuracy, and you can calculate it from a test's precision and recall. Recall, as explained earlier, is true positive divided by the sum of true positive and false negative and precision, as we have seen, is true positive divided by sum of true positive and false positive (Obi et al., 2023) It is for this reason that the F1-score considers false positive and false negative. F1-score is preferred over accuracy especially where there is cost or uneven classes are present. Accuracy is preferred when the false positive and false negative are equally costly. Symbolically in Equation (2),

$$F1\ Score = \frac{2\times Precision \times Recall}{Precision + Recall} \tag{2}$$

In addition to the general assessment of the models, we used recall, specificity, precision, and negative predictive value (NPV) to analyze the ability of the models to detect particular classes. Equations 3-6 present the sensitivity, specificity, precision, and NPV formulae.

Recall

Known as sensitivity or true positive rate, is the ability of a model to find all relevant cases (find true positive) (Obi et al., 2023). It is a mathematically defined in Equation (3),

$$Recall = \frac{TP}{TP+FN} \tag{3}$$

Specificity

A rate that tells us how many true negatives were correctly identified as negatives by a particular classifier. For example, suppose we have a model for classifying headache (positives) vs no-headache (negatives). In general, if the specificity is high, there is a good model, since it separates people without disease from those with the disease (Obi et al., 2023). Symbolically defined in Equation (4),

$$Specificity = \frac{TN}{TN+FP} \quad (4)$$

Precision

Known as Positive Predictive Value is a ratio of true positive divided by all the positives that were observed. We have true positives found (TP) and true negatives incorrectly classified as positives (FP); all of the positives here (Obi et al., 2023). Symbolically defined in Equation (5),

$$Precision\ (PPV) = \frac{TP}{TP+FP} \quad (5)$$

Negative Predictive Value (NPV)

Is the proportion of cases predicted by a model to be negative that are indeed negative. It assesses how trustworthy the model's negative predictions are. The NPV is calculated by the following formula in Equation (6),

True Negatives (TN): Cases that were accurately predicted as negative.
False Negatives (FN): Predicted Negative but are actually Positive.

$$NPV = \frac{TN}{TN+FN} \quad (6)$$

CHAPTER VI
Results and Discussion

This chapter presents the experiments and their results carried out for the evaluation of the system, comparison analysis and the discussion about advantages and limitations of the thesis is explained in this chapter.

Results

The results for each fold of the models are presented in Tables 1-3. However, the mean scores are considered for the final evaluation of the models.

In the first experiment, demonstrates strong and consistent performance for most metrics, as shown in Table 1. The average accuracy and specificity of the model is 96.36% and 98.59%, respectively, which are both proficient in correctly classifying positive and negative cases. As the average AUC is 98.15%, demonstrating very good discriminatory power. Although, we notice a certain variability in recall (sensitivity) which, after three folds, has a lowest value of 71.64% in Fold 2 and a highest value of 91.67% in Fold 4, giving us a mean of 80.76%. Positive Predictive Value (PPV) is relatively stable, with an average of 89.10% and the highest value found in Fold 2 (96.00%). Negative predictive value (NPV) consistently strong and its average across folds is 97.30%. The F1-score balances precision and recall at 84.51% which is a good value for overall performance.

Table 1. Fold results for DenseNet201.

Fold	Accuracy	Recall	Specificity	PPV	NPV	F1-Score	AUC
1	0.9720	0.8421	0.9887	0.9057	0.9799	0.8727	0.9896
2	0.9581	0.7164	0.9954	0.9600	0.9579	0.8205	0.9718
3	0.9600	0.8485	0.9770	0.8485	0.9770	0.8485	0.9754
4	0.9820	0.9167	0.9930	0.9565	0.9861	0.9362	0.9941
5	0.9460	0.7143	0.9752	0.7843	0.9644	0.7477	0.9764
Average	0.9636	0.8076	0.9859	0.8910	0.9730	0.8451	0.9815

The EfficientNetB0 performs relatively stable in almost all metrics as presented in Table 2, as part of this experiment. The model achieves an average accuracy 95.84% of positive cases with a specificity of 97.99%, signifying reliable negative case classification. The AUC is particularly high, with an average AUC of 98.01%, indicating strong overall discriminatory ability. Variability is observed in recall, with the lowest value recorded in Fold 5 (71.43%) to the highest in Fold 3 (89.39%) with a combined average of 80.73%. Similarly, Precision (PPV) varies from Fold 4, with the highest value of 92.65%, to Fold 5 with the value of 75.47%, leading to a mean of 85.09%. The F1-score balances these metrics to 82.71%, and the highest value in Fold 4 is noted (90.00%). The negative predictive value (NPV) across all folds is also strong, with an average of 97.28%.

Table2. Fold results for EfficientNetB0.

Fold	Accuracy	Recall	Specificity	PPV	NPV	F1-Score	AUC
1	0.9580	0.8070	0.9774	0.8214	0.9752	0.8142	0.9894
2	0.9561	0.7463	0.9885	0.9091	0.9619	0.8197	0.9762
3	0.9640	0.8939	0.9747	0.8429	0.9837	0.8676	0.9757
4	0.9720	0.8750	0.9883	0.9265	0.9792	0.9000	0.9940
5	0.9420	0.7143	0.9707	0.7547	0.9642	0.7339	0.9655
Average	0.9584	0.8073	0.9799	0.8509	0.9728	0.8271	0.9801

In this experiment, presents stable performance across most metrics as shown in Table 3. The model has achieved average accuracy of 95.68% and 98.31% of specificity indicating good classification ability in both positive and negative cases. The AUC was also quite impressive, in fact the average AUC was 97.20%, showing excellent model discriminatory power. A slight variation can be observed in recall (sensitivity)amongst folds with 70.15% being resulted in Fold 2 and 82.14% in Fold 5, thus totaling an average result of 77.94%. Precision (PPV) depends too, with a maximum value of 98.21% in Fold 4 and a minimum of 77.05% in Fold 2 (mean 87.19%). The F1-score is 82.17% which balances all these variations with the best score obtained in Fold 4 (85.94%).

Table3.Fold results for ResNet101.

Fold	Accuracy	Recall	Specificity	PPV	NPV	F1-Score	AUC
1	0.9680	0.8070	0.9887	0.9020	0.9755	0.8519	0.9917
2	0.9321	0.7015	0.9677	0.7705	0.9545	0.7344	0.9187
3	0.9600	0.8030	0.9839	0.8833	0.9705	0.8413	0.9799
4	0.9640	0.7639	0.9977	0.9821	0.9617	0.8594	0.9921
5	0.9600	0.8214	0.9775	0.8214	0.9775	0.8214	0.9779
Average	0.9568	0.7794	0.9831	0.8719	0.9679	0.8217	0.9720

The EfficientNetB0 obtained similar results with ResNet101; however, these models' ability to detect positive and negative cases was different. The EfficientNetB0 model obtained a higher recall (sensitivity) result (0.8073) than the ResNet101 model (0.7794) by detecting a higher number of positive cases; however, the ResNet101 model was more capable of correctly classifying the negative cases with a 0.9831 specificity. Even though the sensitivity results of all models were low, the DenseNet model achieved the highest sensitivity (0.8076) and specificity (0.9859). Similarly, the DenseNet201 model achieved the highest PPV and NPV results, which provided more consistent predictions for the dataset.

When the models are compared for the general detection ability for the ICH, the DenseNet201 achieved the highest F1 and AUC scores (0.8451 and 0.9815) and outperformed other models. Table 4 presents the obtained results of this thesis in detail. Figure 4 presents the ROC curves of all models and folds.

In this thesis, DenseNet201, EfficientNetB0, and ResNet101 showed the most alike and sustained performances concerning different metrics. DenseNet201 showed a high average accuracy of 96.36%, a mean specificity of 98.59% and a high AUC of 98.15%. For recall, we noticed some variance from fold to fold with a low of 71.64% in Fold 2 to a high of 91.67% in Fold 4 yielding a mean of 80.76%. This average F1-score of 84.51% is indicant of balanced performance. An average of 95.84% overall accuracy, 97.99% specificity, and 98.01% AUC were reached with EfficientNetB0 as well. Mean recall was 80.73%, ranging from 71.43% (Fold 5) to 89.39 (Fold 3). The F1-score average was 82.71%, with a maximum value of 90.00% in Fold 4.

ResNet101 yielded good result with 95.68% average accuracy, 98.31% specificity and an AUC of 97.20% The recall ranged from 70.15% (Fold 2) to 82.14% (Fold 5), with a mean of 77.94%. F1-score averaged 82.17% with the highest found in Fold 4 (85.94%).

Table 4. Mean results obtained for each model.

Model	Accuracy	Recall	Specificity	PPV	NPV	F1-Score	AUC
DenseNet201	0.9636	0.8076	0.9859	0.8910	0.9730	0.8451	0.9815
EfficientNet B0	0.9584	0.8073	0.9799	0.8509	0.9728	0.8271	0.9801
ResNet 101	0.9568	0.7794	0.9831	0.8719	0.9679	0.8217	0.9720

The ROC curve (Receiver operating characteristic)

Is a statistical tool used to evaluate the performance of binary classifiers by plotting true positive rates against false positive rates as showen in figuer 13. It helps gauge the ability of a classifier while considering confounding variables for better calibration (Machado e Costa et al., 2021). And that can be simply defined as a plot of (F P F), (1- specificity) and (T P F) (Sensitivity) pairs obtained by calculating for varying values of threshold c as (x,y) axis respectively.

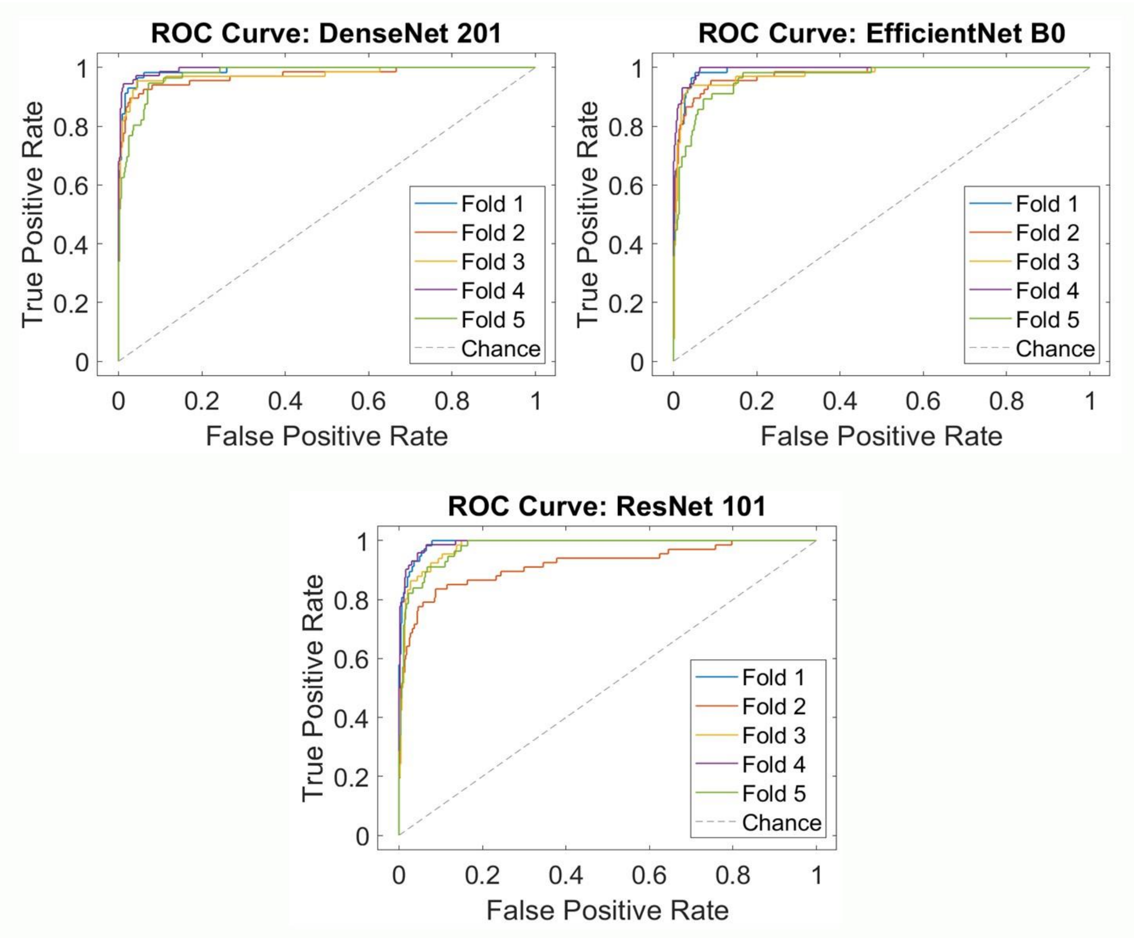

Fig. 13. ROC curves of models for each fold.

Figure 14 shows the confusion matrices obtained from all folds for all models.

The considered pretrained models achieved reasonable results in terms of general detection ability, which provide effective distinguishment of the negative and positive cases. However, it was observed that the models require improvements in detecting positive cases due to the lower number of training images for ICH-positive cases. This could be overcome by applying data augmentation to the positive class in order to increase the training samples; however, scientists have different opinions about the positive effect of data augmentation in the generalization.

Even though the DenseNet201 obtained superior results, it is clear that the clinical use of deep learning systems requires more investigation using different datasets with external validation sets.

The abovementioned problems and challenges are the primary limitations of this thesis.

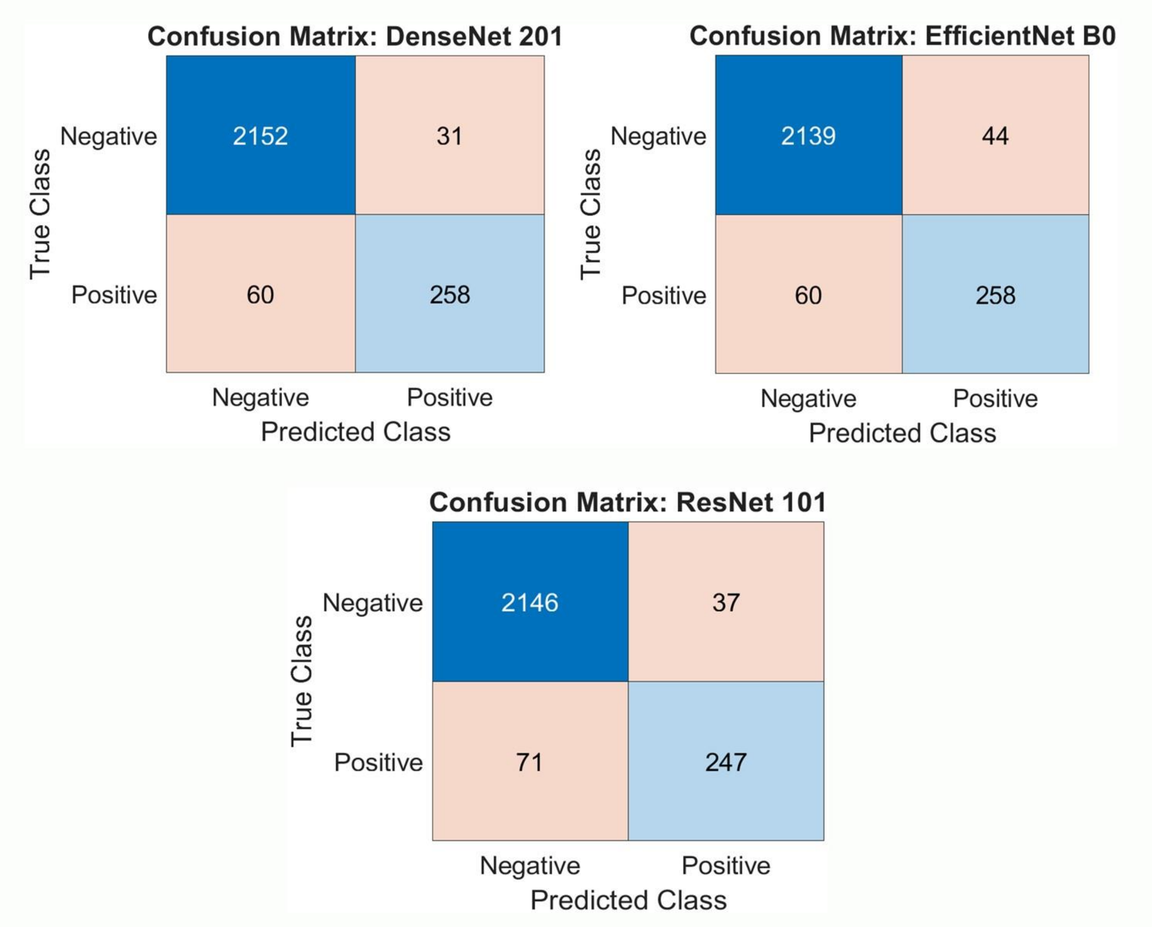

Fig. 14. Confusion matrices obtained in this thesis.

Grad-CAMs

Are class activation maps generated using gradients to highlight important features in neural network predictions (Buono et al., 2024). As showen in figuer 15. CAM(s) are computed by looking at the feature maps and yields per-instance, class-specific attention maps, that highlight important regions of the original input that influenced the classifier (Selvaraju et al., 2020). Following this idea, Grad-CAM and its variants recover from the raw formula by calculating the linear weights as the average of backpropagated gradients of target class for each feature map. With this generalization, one can use the method and apply it to the model without any changes or retraining (Simonyan et al., 2013).

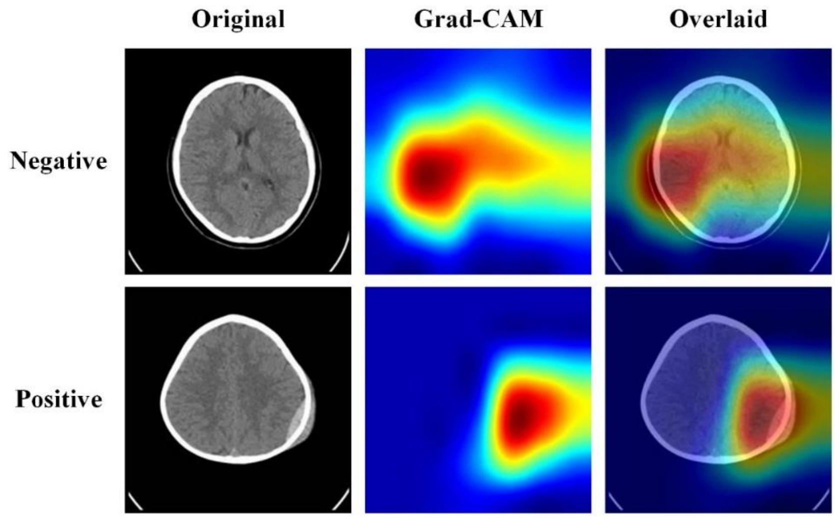

Fig. 15. Grad-CAMs obtained from the superior model.

Discussions

The challenge to accurately differentiate the hemorrhages in the CT images arises when the hemorrhages are subtle, and are using low contrast or features that are difficult to identify. Such challenges emphasize the need of using advanced deep learning architectures for accurate classification and diagnosis.

The use of pretrained models (DenseNet201, EfficientNetB0, and ResNet101) in this study allowed robust feature extraction from CT images. All models had their distinguishing qualities with DenseNet201's improvement of information flow and feature reuse through dense connectivity, EfficientNetB0's effective architecture balancing between accuracy and other resources, and ResNet101's residual connections addressing the vanishing gradient problem. This performance is in fact enabled by its superior ability to classify ICH cases accurately, with DenseNet201 reflected the best results (accuracy of 96.36%, with sensitivity of 80.76% and AUC of 98.15%).

In this thesis, no data augmentation was performed, which preserved the integrity of the initial dataset, however, this might have affected the ability of the models to generalize to unseen data. Nonetheless, with transfer learning, the models were able to learn from images from the ImageNet dataset, further increasing their performance, dataset of 2,500 CT images. Additionally, the 5-fold cross-validation method applied provided strong validation and prevented the model from overfitting.

Highlights One of the key findings is models, especially DenseNet201, can balance sensitivity and specificity. Although sensitivity was comparatively lower, all models achieved high specificity (~99%), indicating that there is still room for improvement in the detection of positive cases. This is fundamentally due to the class imbalance in the dataset where only 318 positive classes are present in the 2500 images. Complimentary techniques such as data augmentation or oversampling for this imbalance could have further increased the models' sensitivity.

A further important observation is the efficiency of the models. EfficientNetB0 is computationally efficient, therefore, can facilitate real-time application of clinical where speed and low resource consumption is needed. Its relatively inferior performance metrics when compared to DenseNet201 would make it a stronger complimentary tool as opposed to a standalone solution for ICH detection.

The research also noted restrictions within the dataset and model structure. Finally, as the publicly available dataset includes only single-modality CT images, models trained on it cannot generalize to other imaging modalities or to multi-class classification problems. Also, the lack of clinical and demographic data limits the diagnostic capacity of the models. Future work should investigate combining multi-modal imaging data and clinical data to further enhance diagnostic performance.

Additionally, the nominated system does not facilitate mini case, such as, with more than one visible hemorrhagic area, or multiple hemorrhagic regions appearing in only a few pixels. This limitation can be addressed by developing sophisticated localization methods to recognize multiple areas of a single image. Thus, the outcome of this study indicates that pretrained deep learning models can really help to improve the performance of ICH detection in CT images. Specifically, DenseNet201 demonstrated the best ability for accurate and robust classification. The result reveals the need for such experiments rigorously considering data flaws and with regards to decision support in a multi-modal clinical setting.

CHAPTER VII

Conclusion

Intracranial hemorrhage is life-threatening and vital if it cannot be detected early. The diagnosis and detection of ICH rely on CT scans; however, indistinct patterns in the images might prevent accurate diagnosis, particularly in regions lacking expert personnel. Therefore, the use of an AI-based system could help with the rapid and accurate detection of ICH.

In this thesis, three pretrained deep learning models, EfficientNetB0, DenseNet201, and ResNet101, were implemented and trained using a transfer learning approach to detect ICH. The results were analyzed using several evaluation metrics.

The DenseNet201 showed superior performance than other models and outperformed other models. The results showed that deep learning models can accurately determine negative cases. However, further improvements are required to increase the recall, which is crucial in preventing mortality. The release of more comprehensive and balanced datasets might provide more comprehensive detection and analysis of the ICH.

Our future work will include combining different datasets to overcome challenges created by different data sources. Additionally, we aim to develop a multi-modal model to combine the demographic or histological information of the patients to improve the recall (sensitivity) of the models.

References

Abrigo, J. M., Ka-long, K., Chen, Q., Lai, B. M., Cheung, T. C., Chu, W. C., & Simon, C. H. (2023). Artificial intelligence for detection of intracranial haemorrhage on head computed tomography scans: diagnostic accuracy in Hong Kong. *Hong Kong Medical Journal*, *29*(2), 112.

Agrawal, D., Poonamallee, L., & Joshi, S. (2023). Automated detection of intracranial hemorrhage from head CT scans applying deep learning techniques in traumatic brain injuries: A comparative review. *Indian Journal of Neurotrauma*.

Alex Krizhevsky, Sutskever, I., & Hinton, G. E. (2012). Imagenet classification with deep convolutional neural networks. *Advances in neural information processing systems*, *25*.

Alexey Dosovitskiy, Springenberg, J. T., Brox, T., & Riedmiller, M. (2014). Striving for simplicity: The all convolutional net. *arXiv preprint arXiv:1412.6806*.

Aloysius, N., & Geetha, M. (2017, April). A review on deep convolutional neural networks. In *2017 international conference on communication and signal processing (ICCSP)* (pp. 0588-0592). IEEE.

Alshazly, H., Linse, C., Abdalla, M., Barth, E., & Martinetz, T. (2021). COVID-Nets: deep CNN architectures for detecting COVID-19 using chest CT scans. *PeerJ Computer Science*, *7*, e655.

Alzubaidi, L., Zhang, J., Humaidi, A. J., Al-Dujaili, A., Duan, Y., Al-Shamma, O., ... & Farhan, L. (2021). Review of deep learning: concepts, CNN architectures, challenges, applications, future directions. *Journal of big Data*, *8*, 1-74.

Anusha Bai, R., & Sangeetha, V. (2023, April). A Comparative Study on Brain Intracerebral Hemorrhage Classification Using Head CT Scan for Stroke Analysis. In *International Conference on Soft Computing for Security Applications* (pp. 633-649). Singapore: Springer Nature Singapore.

Bahrami, M., Keyhanifard, M., & Afzali, M. (2022). Spontaneous intracerebral hemorrhage, initial computed tomography (CT) scan findings, clinical manifestations and possible risk factors. *American Journal of Nuclear Medicine and Molecular Imaging*, *12*(3), 106.

Barman, S., Farid, F. A., Raihan, J., Khan, N. A., Hafiz, M. F. B., Bhattacharya, A., ... & Mansor, S. (2024). Optimized crop disease identification in Bangladesh: A deep learning and SVM hybrid model for rice, potato, and corn. *Journal of Imaging*, *10*(8), 183.

Bishop, C. M., & Nasrabadi, N. M. (2006). *Pattern recognition and machine learning* (Vol. 4, No. 4, p. 738). New York: springer.

Buono, V., Mashhadi, P. S., Rahat, M., Tiwari, P., & Byttner, S. (2024). Expected Grad-CAM: Towards gradient faithfulness. *arXiv preprint arXiv:2406.01274*.

C, Szegedy, Vanhoucke, V., Ioffe, S., Shlens, J., & Wojna, Z. (2016). Rethinking the inception architecture for computer vision. In *Proceedings of the IEEE conference on computer vision and pattern recognition* (pp. 2818-2826).

C. Szegedy, W. Liu, Y. Jia, P. Sermanet, S. Reed, Going deeper with convolutions, CoRR, 2014.

Carhuapoma, J. R., Mayer, S. A., & Hanley, D. F. (Eds.). (2009). *Intracerebral hemorrhage*. Cambridge University Press.

Chang, P. D., Kuoy, E., Grinband, J., Weinberg, B. D., Thompson, M., Homo, R., ... & Chow, D. (2018). Hybrid 3D/2D convolutional neural network for hemorrhage evaluation on head CT. *American Journal of Neuroradiology*, *39*(9), 1609-1616.

Charidimou, A., Shoamanesh, A., Wilson, D., Gang, Q., Fox, Z., Jaeger, H. R., ... & Werring, D. J. (2015). Cerebral microbleeds and postthrombolysis intracerebral hemorrhage risk: updated meta-analysis. *Neurology*, *85*(11), 927-934.

Chen, J., Zeng, Z., Fang, Z., Ma, F., Lv, M., & Zhang, J. (2023). Risk factors for thrombolysis-related intracranial hemorrhage: a systematic review and meta-analysis. *Thrombosis Journal*, *21*(1), 27.

Cheng, J., Gao, K., & Zhou, L. (2023, April). Study of intracranial haematoma localisation based on improved RetinaNet. In *Proceedings of the 2023 8th International Conference on Multimedia and Image Processing* (pp. 73-78).

Chu, S. Y., & Hwang, D. Y. (2016, June). Predicting outcome for intracerebral hemorrhage patients: current tools and their limitations. In *Seminars in Neurology* (Vol. 36, No. 03, pp. 254-260). Thieme Medical Publishers.

Claassen, J., & Park, S. (2022). Spontaneous subarachnoid haemorrhage. *The Lancet*, *400*(10355), 846-862.

Cortés-Ferre, L., Gutiérrez-Naranjo, M. A., Egea-Guerrero, J. J., Pérez-Sánchez, S., & Balcerzyk, M. (2023). Deep learning applied to intracranial hemorrhage detection. *Journal of Imaging*, *9*(2), 37.

Duperron, M. G., Tzourio, C., Schilling, S., Zhu, Y. C., Soumare, A., Mazoyer, B., & Debette, S. (2019). High dilated perivascular space burden: a new MRI marker for risk of intracerebral hemorrhage. *Neurobiology of aging*, *84*, 158-165.

Emberson, J., Lees, K. R., Lyden, P., Blackwell, L., Albers, G., Bluhmki, E., ... & Hacke, W. (2014). Effect of treatment delay, age, and stroke severity on the effects of intravenous thrombolysis with alteplase for acute ischaemic stroke: a meta-analysis of individual patient data from randomised trials. *The Lancet*, *384*(9958), 1929-1935.

Fischbein, N. J., & Wijman, C. A. (2010). Nontraumatic intracranial hemorrhage. *Neuroimaging Clinics*, *20*(4), 469-492.

G. E, Hinton. (2012). Improving neural networks by preventing co-adaptation of feature detectors. *arXiv preprint arXiv:1207.0580*.

Gage, F. H. (2000). Mammalian neural stem cells. *Science*, *287*(5457), 1433-1438.

Gao Huang., Liu, Z., Van Der Maaten, L., & Weinberger, K. Q. (2017). Densely connected convolutional networks. In *Proceedings of the IEEE conference on computer vision and pattern recognition* (pp. 4700-4708).

Gibson, E., Georgescu, B., Ceccaldi, P., Trigan, P. H., Yoo, Y., Das, J., ... & Lui, Y. W. (2022). Artificial intelligence with statistical confidence scores for detection of acute or subacute hemorrhage on noncontrast CT head scans. *Radiology: Artificial Intelligence*, *4*(3), e210115.

Gong, Y., Wang, L., Guo, R., & Lazebnik, S. (2014). Multi-scale orderless pooling of deep convolutional activation features. In *Computer Vision–ECCV 2014: 13th European Conference, Zurich, Switzerland, September 6-12, 2014, Proceedings, Part VII 13* (pp. 392-407). Springer International Publishing.

He, K., Zhang, X., Ren, S., & Sun, J. (2016). Deep residual learning for image recognition. In *Proceedings of the IEEE conference on computer vision and pattern recognition* (pp. 770-778).

Hsieh, W., Bi, Z., Liu, J., Peng, B., Zhang, S., Pan, X., ... & Liu, M. (2024). Deep Learning, Machine Learning--Digital Signal and Image Processing: From Theory to Application. *arXiv preprint arXiv:2410.20304*.

Hssayeni, M., Croock, M., Salman, A., Al-khafaji, H., Yahya, Z., & Ghoraani, B. (2020). Computed tomography images for intracranial hemorrhage detection and segmentation. *Intracranial hemorrhage segmentation using a deep convolutional model. Data*, *5*(1), 14.

Huang, G., Liu, Z., Van Der Maaten, L., & Weinberger, K. Q. (2017). Densely connected convolutional networks. In *Proceedings of the IEEE conference on computer vision and pattern recognition* (pp. 4700-4708).

Ioffe, S. (2015). Batch normalization: Accelerating deep network training by reducing internal covariate shift. *arXiv preprint arXiv:1502.03167*.

Jaenisch, R., & Young, R. (2008). Stem cells, the molecular circuitry of pluripotency and nuclear reprogramming. *Cell*, *132*(4), 567-582.

Jégou, S., Drozdzal, M., Vazquez, D., Romero, A., & Bengio, Y. (2017). The one hundred layers tiramisu: Fully convolutional densenets for semantic segmentation. In *Proceedings of the IEEE conference on computer vision and pattern recognition workshops* (pp. 11-19).

K. He., Zhang, X., Ren, S., & Sun, J. (2016). Deep residual learning for image recognition. In *Proceedings of the IEEE conference on computer vision and pattern recognition* (pp. 770-778).

Kalshetty, R., & Parveen, A. (2023). Abnormal event detection model using an improved ResNet101 in context aware surveillance system. *Cognitive Computation and Systems*, *5*(2), 153-167.

Karki, M., Cho, J., Lee, E., Hahm, M. H., Yoon, S. Y., Kim, M., ... & Park, S. (2020). CT window trainable neural network for improving intracranial hemorrhage detection by combining multiple settings. *Artificial Intelligence in Medicine*, *106*, 101850.

Kidwell, C. S., Chalela, J. A., Saver, J. L., Starkman, S., Hill, M. D., Demchuk, A. M., ... & Warach, S. (2004). Comparison of MRI and CT for detection of acute intracerebral hemorrhage. *Jama*, *292*(15), 1823-1830.

Kimura, K., Minematsu, K., & Yamaguchi, T. (2005). Atrial fibrillation as a predictive factor for severe stroke and early death in 15 831 patients with acute ischaemic stroke. *Journal of Neurology, Neurosurgery & Psychiatry*, *76*(5), 679-683.

Kobata, H., & Ikeda, N. (2021). Recent updates in neurosurgical interventions for spontaneous intracerebral hemorrhage: minimally invasive surgery to improve surgical performance. *Frontiers in Neurology*, *12*, 703189.

Kranz, P. G., Malinzak, M. D., & Amrhein, T. J. (2018). Approach to imaging in patients with spontaneous intracranial hemorrhage. *Neuroimaging Clinics*, *28*(3), 353-374.

Kulesh, A. A. (2020). Current approaches to diagnosing in intracerebral hemorrhage. *Neurology, Neuropsychiatry, Psychosomatics*, *12*(2), 4-11.

Kumar, H., Virmani, A., Tripathi, S., Agrawal, R., & Kumar, S. (2021). Transfer learning and supervised machine learning approach for detection of skin cancer: performance analysis and comparison. *Transfer*, *10*(1).

Kuo, W., Häne, C., Mukherjee, P., Malik, J., & Yuh, E. L. (2019). Expert-level detection of acute intracranial hemorrhage on head computed tomography using deep learning. *Proceedings of the National Academy of Sciences*, *116*(45), 22737-22745.

LeCun, Y., Bengio, Y., & Hinton, G. (2015). Deep learning. *nature*, *521*(7553), 436-444.

LeCun, Y., Boser, B., Denker, J., Henderson, D., Howard, R., Hubbard, W., & Jackel, L. (1989). Handwritten digit recognition with a back-propagation network. *Advances in neural information processing systems*, *2*.

LeCun, Y., Bottou, L., Bengio, Y., & Haffner, P. (1998). Gradient-based learning applied to document recognition. *Proceedings of the IEEE*, *86*(11), 2278-2324.

Lee, S. H. (2018). Symptoms and signs of hemorrhagic stroke. *Stroke Revisited: Hemorrhagic Stroke*, 103-108.

Li, L., Wei, M., Liu, B. O., Atchaneeyasakul, K., Zhou, F., Pan, Z., ... & Scalzo, F. (2020). Deep learning for hemorrhagic lesion detection and segmentation on brain CT images. *IEEE journal of biomedical and health informatics*, *25*(5), 1646-1659.

Li, Y., Wu, J., Li, H., Li, D., Du, X., Chen, Z., ... & Hu, Q. (2012). Automatic detection of the existence of subarachnoid hemorrhage from clinical CT images. *Journal of medical systems*, *36*, 1259-1270.

Ljungqvist, J., Candefjord, S., Persson, M., Jönsson, L., Skoglund, T., & Elam, M. (2017). Clinical evaluation of a microwave-based device for detection of traumatic intracranial hemorrhage. *Journal of neurotrauma*, *34*(13), 2176-2182.

Machado e Costa, F., & Braga, A. C. (2021, September). Exploring Methodologies for ROC Curve Covariate Study with R. In *International Conference on*

Computational Science and Its Applications (pp. 563-576). Cham: Springer International Publishing.

MacIntosh, B. J., Liu, Q., Schellhorn, T., Beyer, M. K., Groote, I. R., Morberg, P. C., ... & Bjørnerud, A. (2023). Radiological features of brain hemorrhage through automated segmentation from computed tomography in stroke and traumatic brain injury. *Frontiers in Neurology*, *14*, 1244672.

Majeed, M. A. A., Al Okashi, O. M., & Alrawi, A. T. (2023, January). Intracranial hemorrhage detection and classification from CT images based on multiple features and machine learning approaches. In *2023 15th International Conference on Developments in eSystems Engineering (DeSE)* (pp. 498-503). IEEE.

Meng, F., Wang, J., Zhang, H., & Li, W. (2022). [Retracted] Artificial Intelligence-Enabled Medical Analysis for Intracranial Cerebral Hemorrhage Detection and Classification. *Journal of healthcare engineering*, *2022*(1), 2017223.

Messé, S. R., Pervez, M. A., Smith, E. E., Siddique, K. A., Hellkamp, A. S., Saver, J. L., ... & Schwamm, L. H. (2013). Lipid profile, lipid-lowering medications, and intracerebral hemorrhage after tPA in Get With The Guidelines–Stroke. *Stroke*, *44*(5), 1354-1359.

Minfei, L., Yidong, G., Ze, C., Zhi, W., Erik, S., & Branko, Š. (2022). Microstructure-informed deep convolutional neural network for predicting short-term creep modulus of cement paste. *Cement and Concrete Research*, *152*, 106681.

Mohammed, B. A., Senan, E. M., Al-Mekhlafi, Z. G., Rassem, T. H., Makbol, N. M., Alanazi, A. A., ... & Sallam, A. A. (2022). Multi-method diagnosis of CT images for rapid detection of intracranial hemorrhages based on deep and hybrid learning. *Electronics*, *11*(15), 2460.

Mohammed, B. A., Senan, E. M., Al-Mekhlafi, Z. G., Rassem, T. H., Makbol, N. M., Alanazi, A. A., ... & Sallam, A. A. (2022). Multi-method diagnosis of CT images for rapid detection of intracranial hemorrhages based on deep and hybrid learning. *Electronics*, *11*(15), 2460.

Mucha, S., & Babu, A. R. (2024). Classification of intracranial hemorrhage (CT) images using CNN-LSTM method and image-based GLCM features. In *MATEC Web of Conferences* (Vol. 392, p. 01075). EDP Sciences.

Nguyen, A., Yosinski, J., & Clune, J. (2015). Deep neural networks are easily fooled: High confidence predictions for unrecognizable images. In *Proceedings of the IEEE conference on computer vision and pattern recognition* (pp. 427-436).

Nizarudeen, S., & Shunmugavel, G. R. (2022, November). Intracranial Hemorrhage Grading using Novel ConceptionNet. In *2022 IEEE 19th India Council International Conference (INDICON)* (pp. 1-6). IEEE.

O. Rippel, Snoek, J., & Adams, R. P. (2015). Spectral representations for convolutional neural networks. *Advances in neural information processing systems*, *28*.

O'Carroll, C. B., Brown, B. L., & Freeman, W. D. (2021, June). Intracerebral hemorrhage: a common yet disproportionately deadly stroke subtype. In *Mayo Clinic Proceedings* (Vol. 96, No. 6, pp. 1639-1654). Elsevier.

Obi, J. C. (2023). A comparative study of several classification metrics and their performances on data. *World Journal of Advanced Engineering Technology and Sciences*, *8*(1), 308-314.

Ozsahin, I., Sekeroglu, B., & Butler, T. (2021). Classification of Alzheimer's disease by using tau PET images and deep convolutional neural networks. *Alzheimer's & Dementia*, *17*, e049148.

Pamela, W Schaefer., & Edjlali, M. (2024). Nontraumatic Intracranial Hemorrhage. *Diseases of the Brain, Head and Neck, Spine 2024-2027: Diagnostic Imaging*, 49-68.

Phung Rhee, E. J. (2018). A deep learning approach for classification of cloud image patches on small datasets.

Piao, Z., Gu, Y. H., Jin, H., & Yoo, S. J. (2023). Intracerebral hemorrhage CT scan image segmentation with HarDNet based transformer. *Scientific Reports*, *13*(1), 7208.

Rashid, M. H. O., & Ahmed, B. (2023, May). Recognition of Intracranial Hemorrhage with its Subtypes from CT Images using Deep Learning Approach. In *2023 7th International Conference on Intelligent Computing and Control Systems (ICICCS)* (pp. 372-375). IEEE.

Remedios, S. W., Roy, S., Bermudez, C., Patel, M. B., Butman, J. A., Landman, B. A., & Pham, D. L. (2020). Distributed deep learning across multisite datasets for generalized CT hemorrhage segmentation. *Medical physics*, *47*(1), 89-98.

Rguibi, Z., Hajami, A., Zitouni, D., Elqaraoui, A., & Bedraoui, A. (2022). Cxai: Explaining convolutional neural networks for medical imaging diagnostic. *Electronics*, *11*(11), 1775.

Sacco, S., Marini, C., Toni, D., Olivieri, L., & Carolei, A. (2009). Incidence and 10-year survival of intracerebral hemorrhage in a population-based registry. *Stroke*, *40*(2), 394-399.

Sanner, A. P., Grauhan, N. F., Meyer, M., Leukert, L., Brockmann, M. A., Othman, A. E., & Mukhopadhyay, A. (2024, December). Detection of Intracranial Hemorrhage for Trauma Patients. In *International Conference on Pattern Recognition* (pp. 1-14). Cham: Springer Nature Switzerland.

Selvaraju, R. R., Cogswell, M., Das, A., Vedantam, R., Parikh, D., & Batra, D. (2020). Grad-CAM: visual explanations from deep networks via gradient-based localization. *International journal of computer vision*, *128*, 336-359.

Sengupta, J., & Alzbutas, R. (2022). Intracranial hemorrhages segmentation and features selection applying cuckoo search algorithm with gated recurrent unit. *Applied Sciences*, *12*(21), 10851.

Sengupta, J., Alzbutas, R., Falkowski-Gilski, P., & Falkowska-Gilska, B. (2023). Intracranial hemorrhage detection in 3D computed tomography images using a bi-directional long short-term memory network-based modified genetic algorithm. *Frontiers in neuroscience*, *17*, 1200630.

Simonyan, K., Vedaldi, A., & Zisserman, A. (2013). Deep inside convolutional networks: Visualising image classification models and saliency maps. *arXiv preprint arXiv:1312.6034*.

Szegedy, C., Ioffe, S., Vanhoucke, V., & Alemi, A. (2017, February). Inception-v4, inception-resnet and the impact of residual connections on learning. In *Proceedings of the AAAI conference on artificial intelligence* (Vol. 31, No. 1).

Tan, M., & Le, Q. (2019, May). Efficientnet: Rethinking model scaling for convolutional neural networks. In *International conference on machine learning* (pp. 6105-6114). PMLR.

Thalhammer, J., Schultheiss, M., Dorosti, T., Lasser, T., Pfeiffer, F., Pfeiffer, D., & Schaff, F. (2023). Improving automated hemorrhage detection in sparse-view computed tomography via deep convolutional neural network based artifact reduction. *arXiv preprint arXiv:2303.09340*.

Vespa, P., Hanley, D., Betz, J., Hoffer, A., Engh, J., Carter, R., ... & Martin, N. (2016). ICES (Intraoperative Stereotactic Computed Tomography-Guided Endoscopic Surgery) for brain hemorrhage: a multicenter randomized controlled trial. *Stroke, 47*(11), 2749-2755.

Whiteley, W. N., Emberson, J., Lees, K. R., Blackwell, L., Albers, G., Bluhmki, E., ... & Baigent, C. (2016). Risk of intracerebral haemorrhage with alteplase after acute ischaemic stroke: a secondary analysis of an individual patient data meta-analysis. *The Lancet Neurology*, *15*(9), 925-933.

Whiteley, W. N., Slot, K. B., Fernandes, P., Sandercock, P., & Wardlaw, J. (2012). Risk factors for intracranial hemorrhage in acute ischemic stroke patients treated with recombinant tissue plasminogen activator: a systematic review and meta-analysis of 55 studies. *Stroke, 43*(11), 2904-2909.

Yaghi, S., Willey, J. Z., Cucchiara, B., Goldstein, J. N., Gonzales, N. R., Khatri, P., ... & Schwamm, L. H. (2017). Treatment and outcome of hemorrhagic transformation after intravenous alteplase in acute ischemic stroke: a scientific statement for healthcare professionals from the American Heart Association/American Stroke Association. *Stroke*, *48*(12), e343-e361.

Ye, H., Gao, F., Yin, Y., Guo, D., Zhao, P., Lu, Y., ... & Xia, J. (2019). Precise diagnosis of intracranial hemorrhage and subtypes using a three-dimensional joint convolutional and recurrent neural network. *European radiology*, *29,* 6191-6201.

Yeo, M., Tahayori, B., Kok, H. K., Maingard, J., Kutaiba, N., Russell, J., ... & Asadi, H. (2023). Evaluation of techniques to improve a deep learning algorithm for the automatic detection of intracranial haemorrhage on CT head imaging. *European Radiology Experimental*, *7*(1), 17.

Zahuranec, D. B., Brown, D. L., Lisabeth, L. D., Gonzales, N. R., Longwell, P. J., Smith, M. A., ... & Morgenstern, L. B. (2007). Early care limitations independently predict mortality after intracerebral hemorrhage. *Neurology, 68*(20), 1651-1657.

Zeiler, M. D., & Fergus, R. (2013). Stochastic pooling for regularization of deep convolutional neural networks. *arXiv preprint arXiv:1301.3557*.

Zeiler, M. D., & Fergus, R. (2014). Visualizing and understanding convolutional networks. In *Computer Vision–ECCV 2014: 13th European Conference,* *Zurich, Switzerland, September 6-12, 2014, Proceedings, Part I 13* (pp. 818-833). Springer International Publishing.

Zhang, Y., Zhao, Z. M., Wang, X. C., Feng, H. Q., & Lin, J. (2021). Construction of green tea recognition model based on ResNet convolutional neural network.

Zhou, J. F., Xiong, Y., Kang, X., Pan, Z., Zhu, Q., Goldbrunner, R., ... & Stavrinou, P. (2022). Application of stem cells and exosomes in the treatment of intracerebral hemorrhage: an update. *Stem Cell Research & Therapy*, *13*(1), 281.

Appendices

Appendix A

There is no ethical approval document that can be presented.

Assist. Prof. Dr. Omid MIRZAEI

Supervisor

Appendix B
Similarity Report

Thesis

ORIGINALITY REPORT

15%	11%	10%	5%
SIMILARITY INDEX	INTERNET SOURCES	PUBLICATIONS	STUDENT PAPERS

PRIMARY SOURCES

Assist. Prof. Dr. Omid MIRZAEI

Supervisor